

Partial Path Integration  
of Quantum Fields:  
Two-Loop Analysis of the SU(2)  
Gauge-Higgs Model  
at Finite Temperature

A. Jakovác<sup>1</sup> and A. Patkós<sup>2</sup>  
Department of Atomic Physics  
Eötvös University, Budapest, Hungary

September 10, 2018

**Abstract**

High temperature reduction of the SU(2) Higgs model is realised by partially integrating its partition function. Various approximate forms of the effective theory resulting from the integration over non-static fields and the static electric potential are analysed. Also non-polynomial and non-local terms are allowed. Consistency of the perturbative solution is ensured by new types of induced counterterms. Perturbative phase transition characteristics are presented in the Higgs mass range 30-120 GeV, and compared to results of other perturbative approaches.

---

<sup>1</sup>*e-mail address: jako@hercules.elte.hu, from September 1996: DESY, Theory Group*

<sup>2</sup>*e-mail address: patkos@ludens.elte.hu*

# 1 Introduction

Physical systems develop at finite temperature multiple mass-scales. Decoupling theorems [1] ensure that effective representations can be found for the lighter degrees of freedom at scales asymptotically separated from the heavier scales. The effective couplings can be related to the parameters of the original system by matching values of the same quantities calculated in the effective model and the original model simultaneously [2, 3, 4].

In weakly coupled gauge theories (the class where the electroweak theory belongs to) matching can be performed perturbatively. The simplest is to match the renormalised Green's functions computed in the two theories separately. This tacitly assumes the renormalisability of the effective model. Though at large distances local operators of lower scaling dimensions dominate indeed, it is important to assess quantitatively the rate of suppression of higher dimensional operators.

In finite temperature theories integration over non-static fields yields for static  $n$ -point functions with typical momenta  $\mathcal{O}(p)$ , expressions analytic in  $p^2/M_{heavy}^2$ , therefore the occurring non-localities can always be expanded in a kind of gradient expansion. We shall demonstrate, that in Higgs systems to  $\mathcal{O}(g^4, \lambda g^2, \lambda^2)$  accuracy, the non-local effects in the effective Higgs-potential arising from non-static fields can be represented *exactly* by correcting the coefficient of the term quadratic in the Higgs-field.

Similar conclusions are arrived at when the contribution of non-static modes to higher dimensional (non-derivative) operators is investigated.

The situation changes when a heavy *static* field is integrated out. The contribution to the polarisation functions from this degree of freedom is not analytic neither in  $p^2/M_{heavy}^2$  nor in  $\Phi^2/M_{heavy}^2$ . For the momentum dependence no gradient expansion can be proven to exist. Though the contribution to the effective Higgs-potential can be represented approximately by an appropriately corrected local gauge-Higgs theory, it does not automatically correspond to a systematic weak coupling expansion. Assuming that the important range of variation of the Higgs field is  $\sim gT$ , one proceeds with the expansion, and the validity of this assumption is checked *a posteriori*. In case of strong first order transitions this assumption is certainly incorrect, but seems to be justified for the Standard Model with Higgs masses around 80GeV.

Non-analytic dependence on field variables is reflected in the appearance

of non-polynomial local terms in the reduced effective theory. Consistent treatment of such pieces is an interesting result of our paper (see the discussion of the  $U(1)$  case in [10]).

The method of integration over specific (heavy static and non-static) classes of fields in the path integral (Partial Path Integration, PPI), instead of matching, provides us with a direct method of inducing all non-local and non-polynomial corrections automatically. Though the calculations are much more painful, than those involved in matching, the value of PPI in our eyes is just the possibility of assessing the range of applicability of the technically simpler method.

The explicit expression of the non-local and/or non-polynomial parts of the action and the impact of these terms on the effective finite temperature Higgs-potential will be investigated in the present paper for the  $SU(2)$  gauge-Higgs model. This model is of central physical importance in investigating the nature of the cosmological electroweak phase transition [5]. Earlier, PPI has been applied to the  $O(N)$  model by one of us [6].

A similar, but even more ambitious program is being pursued by Mack and collaborators [7]. They attempt at performing PPI with the goal of deriving in a unique procedure the perfect lattice action of the coarse grained effective model for the light degrees of freedom.

Our calculation stays within the continuum perturbative framework. PPI will be performed with two-loop accuracy for two reasons:

i) The realisation of PPI on Gaussian level does not produce non-local terms, though non-polynomial local terms already do appear. The consistent cut-off independence of the perturbation theory with non-polynomial terms can be tested first in calculations which involve also 2-loop diagrams.

ii) It has been demonstrated that the quantitative non-perturbative characterisation of the effective  $SU(2)$  gauge-Higgs model is sensitive to two-loop corrections of the cut-off (lattice spacing) dependence of its effective bare couplings [8, 9]. We would like to investigate possible variations of the relation of the effective couplings to the parameters of the original theory when the applied regularisation and renormalisation schemes change.

The integration over the non-static and of the heavy static fields will not be separated, but is performed in parallel with help of the thermal counterterm technique already applied in the PPI of the  $U(1)$  Higgs model [10].

The paper is organised in the following way. In section 2 the basic definitions are given and the operational steps involved in the 2-loop PPI are listed.

In Section 3 we are going to discuss the contributions from fully non-static fluctuations. In Section 4 the contribution of the diagrams involving also heavy static propagators is discussed. In both sections particular attention is paid to the analysis of the effective non-local interactions. In Section 5 the effective Higgs potential is calculated from the 2-loop level effective non-local and non-polynomial 3-d (NNA) action with 2-loop accuracy. Also the local polynomial (LPA) and local non-polynomial (LNA) approximations are worked out. The quantitative perturbative characterisation of the phase transition and its comparison with other approaches will be presented in Section 6. Our conclusions are summarised in Section 7. In order to make the paper better readable, the details of the computations discussed in Sections 3 to 5 are relegated to various Appendices.

## 2 Steps of perturbative PPI

The model under consideration is the SU(2) gauge-Higgs model with one complex Higgs doublet:

$$\begin{aligned}\mathcal{L} &= \frac{1}{4}F_{mn}^a F_{mn}^a + \frac{1}{2}(\nabla_m \Phi)^\dagger (\nabla_m \Phi) + \frac{1}{2}m^2 \Phi^\dagger \Phi + \frac{\lambda}{24}(\Phi^\dagger \Phi)^2 + \mathcal{L}_{CT}, \\ F_{mn}^a &= \partial_m A_n^a - \partial_n A_m^a + g\epsilon_{abc}A_m^b A_n^c, \\ \nabla_m &= \partial_m - igA_m^a \tau_a.\end{aligned}\tag{1}$$

The integrations over the non-static Matsubara modes and the static electric component of the vector potential will be performed with two-loop accuracy. In the case of the static electric potential resummed perturbation theory is applied, simply realised by adding the mass term  $(Tm_D^2/2) \int d^3x (A_0^a(\mathbf{x}))^2$  to the free action and compensating for it in the interaction piece. The resummation discriminates between the static and non-static  $A_0$  components, therefore in the Lagrangean density the replacement

$$A_0(\mathbf{x}, \tau) \rightarrow A_0(\mathbf{x}) + a_0(\mathbf{x}, \tau)\tag{2}$$

should be done. (With lower case letters we always refer to non-static fields.)

In the first step we are going to calculate the local (potential) part of the reduced Lagrangean. For this a constant background is introduced into the Higgs-multiplet:

$$\Phi(\mathbf{x}, \tau) = \Phi_0 + \phi(\mathbf{x}, \tau),$$

$$\phi(\mathbf{x}, \tau) = \begin{pmatrix} \xi_4 + i\xi_3 \\ i\xi_1 - \xi_2 \end{pmatrix}, \quad (3)$$

where  $\Phi_0$  was chosen to be the constant counterpart of  $\xi_4$ . The dependence on the other static components is reconstructed by requiring the O(4) symmetry of the potential energy.

In the second step the kinetic piece of the reduced Lagrangean is investigated. In order to fix the coefficient of the conventional kinetic piece to 1/2, one has to rescale the fields. The wave function renormalisation constants should be calculated with  $\mathcal{O}(g)$  accuracy. The derivative part of the scalar action can be extended upon the requirement of spatial gauge invariance to include the magnetic vector-scalar interaction into itself.

Higher derivative contributions to the effective action can be summarized under the common name *non-local* interactions. They appear first in the two-loop calculation of the polarisation functions of the different fields.

The exponent of the functional integration has the following explicit expression:

$$\begin{aligned} \mathcal{L}^{(cl)} + \mathcal{L}^{(2)} = & \frac{1}{2}m^2\Phi_0^2 + \frac{\lambda}{24}\Phi_0^4 \\ & + \frac{1}{2}a_m^a(-K) \left[ \left( K^2 + \frac{g^2}{4}\Phi_0^2 \right) \delta_{mn} - \left( 1 - \frac{1}{\alpha} \right) K_m K_n \right] a_n^a(K) \\ & + \frac{1}{2}A_0^a(-k) \left[ k^2 + \frac{g^2}{4}\Phi_0^2 + m_D^2 \right] A_0^a(k) \\ & + \frac{1}{2}\xi_H(-K) \left[ K^2 + m^2 + \frac{\lambda}{2}\Phi_0^2 \right] \xi_H(K) \\ & + \frac{1}{2}\xi_a(-K) \left[ K^2 + m^2 + \frac{\lambda}{6}\Phi_0^2 \right] \xi_a(K) + c_a^\dagger(K)K^2c_a(K). \quad (4) \end{aligned}$$

where  $c$  denotes the ghost fields, and the notation  $\xi_4 \equiv \xi_H$  has been introduced. Landau gauge fixing and the Faddeev-Popov ghost terms are included. The above expression implies the following propagators for the different fields to be integrated out:

$$\begin{aligned} \langle a_m^a(P)a_n^b(Q) \rangle &= \frac{\delta_{ab}}{P^2 + m_a^2} \left( \delta_{mn} - \frac{P_m P_n}{P^2} \right) \hat{\delta}(P + Q), \quad m_a^2 = \frac{g^2}{4}\Phi_0^2, \\ \langle A_0^a(P)A_0^b(Q) \rangle &= \frac{\delta_{ab}}{P^2 + m_{A0}^2} \hat{\delta}(P + Q), \quad m_{A0}^2 = m_D^2 + \frac{g^2}{4}\Phi_0^2, \end{aligned}$$

$$\begin{aligned}
\langle \xi_H(P) \xi_H(Q) \rangle &= \frac{1}{P^2 + m_H^2} \hat{\delta}(P + Q), & m_H^2 &= m^2 + \frac{\lambda}{2} \Phi_0^2, \\
\langle \xi_a(P) \xi_b(Q) \rangle &= \frac{\delta_{ab}}{P^2 + m_G^2} \hat{\delta}(P + Q), & m_G^2 &= m^2 + \frac{\lambda}{6} \Phi_0^2, \\
\langle c_a^\dagger(P) c_b(Q) \rangle &= -\frac{\delta_{ab}}{P^2} \hat{\delta}(P - Q). & & (5)
\end{aligned}$$

( $\hat{\delta}$  denotes the finite temperature generalisation of Dirac's delta-function.)

The interaction part of the Lagrangean density consists of two parts. In the first set all non-quadratic vertices are collected:

$$\begin{aligned}
\mathcal{L}_I = & ig S_{abc}^{mnl}(P, Q, K) a_m^a(P) a_n^b(Q) a_l^c(K) \\
& + 3ig S_{abc}^{mn0}(P, Q, k) a_m^a(P) a_n^b(Q) A_0^c(k) \\
& + \frac{g^2}{4} \left[ (a_m^a a_m^a)^2 - (a_m^a a_n^a)^2 + 2(A_0^a A_0^a a_i^b a_i^b - A_0^a A_0^a a_i^a a_i^b) \right] \\
& + g^2 (A_0^a a_0^a a_i^b a_i^b - A_0^a a_0^b a_i^a a_i^b) \\
& - i \frac{g}{2} a_m^a(P) ((K - Q)_m \xi_a(Q) \xi_H(K) + \epsilon_{abc} K_m \xi_b(Q) \xi_c(K)) \\
& - i \frac{g}{2} A_0^a(p) ((K - Q)_0 \xi_a(Q) \xi_H(K) + \epsilon_{abc} K_0 \xi_b(Q) \xi_c(K)) \\
& + \frac{g^2}{8} (a_m^a a_m^a + 2A_0^a a_0^a + A_0^a A_0^a) (\xi_H^2 + \xi_a^2) + \frac{g^2}{4} \Phi_0 \xi_H (a_m^a a_m^a + 2A_0^a a_0^a) \\
& + \frac{\lambda}{24} (\xi_H^2 + \xi_a^2)^2 + \frac{\lambda}{6} \Phi_0 \xi_H (\xi_H^2 + \xi_a^2) + ig \epsilon_{abc} P_m c_a^\dagger(P) a_m^b(Q) c_c(K) \\
& + ig \epsilon_{abc} P_0 c_a^\dagger(P) A_0^b(Q) c_c(K), & (6)
\end{aligned}$$

where the symmetrised trilinear coupling is

$$S_{abc}^{mnl}(P, Q, K) = \frac{1}{6} \epsilon_{abc} [(P - Q)_l \delta_{mn} + (Q - K)_m \delta_{nl} + (K - P)_n \delta_{lm}]. \quad (7)$$

The second piece is quadratic and corresponds to the  $T = 0$  and the thermal counterterms:

$$\begin{aligned}
\mathcal{L}_{CT} = & \frac{1}{2} (Z_\Phi \delta m^2 + (Z_\Phi - 1) m^2) \Phi_0^2 + (Z_\Phi^2 Z_\lambda - 1) \frac{\lambda}{24} \Phi_0^4 \\
& + \frac{1}{2} (Z_A - 1) a_m^a \left( K^2 \delta_{mn} - \left( 1 - \frac{1}{\alpha} \right) K_m K_n \right) a_n^a \\
& + \frac{g^2}{8} (Z_A Z_\Phi Z_g^2 - 1) \Phi_0^2 a_m^2 + \frac{1}{2} (Z_A - 1) A_0^a k^2 A_0^a
\end{aligned}$$

$$\begin{aligned}
& + \frac{g^2}{8} (Z_A Z_\Phi Z_g^2 - 1) \Phi_0^2 A_0^2 - \frac{1}{2} m_D^2 A_0^2 \\
& + \frac{1}{2} \xi_H \left( (Z_\Phi - 1)(K^2 + m^2) + Z_\Phi \delta m^2 + (Z_\Phi^2 Z_\lambda - 1) \frac{\lambda}{2} \Phi_0^2 \right) \xi_H \\
& + \frac{1}{2} \xi_a \left( (Z_\Phi - 1)(K^2 + m^2) + Z_\Phi \delta m^2 + (Z_\Phi^2 Z_\lambda - 1) \frac{\lambda}{6} \Phi_0^2 \right) \xi_a \\
& + (Z_c - 1) c_a^\dagger K^2 c_a.
\end{aligned} \tag{8}$$

The multiplicative and additive renormalisation constants are defined from the relations between the renormalised and the bare couplings, as listed next:

$$\begin{aligned}
g_B &= Z_g g, & \lambda_B &= Z_\lambda \lambda, \\
A_B &= Z_A^{1/2} A, & \Phi_B &= Z_\Phi^{1/2} \Phi, \\
c_B &= Z_c c, & m_B^2 &= m^2 + \delta m^2.
\end{aligned} \tag{9}$$

The quadratic approximation to the counterterms is sufficient for our calculation, since they contribute only at one-loop.

The new couplings, emerging after the 4-d ( $T=0$ ) renormalisation conditions are imposed, are finite from the point of view of the 4-d ultraviolet behavior, but should be considered to be the bare couplings of the effective field theory, since they explicitly might depend on the 3-d cut-off.

## 3 Non-static fluctuations

### 3.1 The potential (local) term of the effective action

The 1-loop contribution to the potential energy of a homogenous  $\Phi_0$ -background is expressed through the standard sum-integral (with the  $n = 0$  mode excluded from the sum)

$$I_4(m) = \int'_K \ln(K^2 + m^2). \tag{10}$$

The meaning of the primed integration symbol and the characteristic features of this integral are detailed in Appendix A. Also the counterterms evaluated with the background  $\Phi_0$  belong to the 1-loop potential. The complete 1-loop

expression of the regularised bare potential is given by

$$\begin{aligned}
V_{\mathcal{E}\mathcal{F}}^{(1)} &= \frac{1}{2}\Phi_0^2 \left[ \left( \frac{9g^2}{4} + \lambda \right) \frac{\Lambda^2}{8\pi^2} + \left( \frac{3g^2}{16} + \frac{\lambda}{12} \right) T^2 \right. \\
&\quad \left. - \left( \frac{3g^2}{2} + \lambda \right) \frac{\Lambda T}{2\pi^2} + \left( 1 + 2I_{20}\lambda - \frac{\lambda}{8\pi^2} \ln \frac{\Lambda}{T} \right) m^2 \right] \\
&\quad + \frac{1}{24}\Phi_0^4 \left[ \lambda + \left( \frac{27g^4}{4} + 4\lambda^2 \right) \left( I_{20} - \frac{1}{16\pi^2} \ln \frac{\Lambda}{T} \right) \right] \quad (11)
\end{aligned}$$

(for the meaning of the notation  $I_{20}$ , and others below, see Appendix A). Its temperature independent cut-off dependences are cancelled by appropriately choosing the coefficients of the renormalisation constants in the "classical" counterterm expression:

$$V_{CT}^{(1)} = \frac{1}{2}(\delta m_1^2 + Z_{\Phi_1} m^2)\Phi_0^2 + (2Z_{\Phi_1} + Z_{\lambda_1})\frac{\lambda}{24}\Phi_0^4. \quad (12)$$

The list of two-loop diagrams and the algebraic expressions for each of them is the same as in case of the effective potential calculation. They appear in several papers [11, 12] in terms of two standard sum-integrals, in addition to the  $I_4$  function defined above. These functions in the present case are analytic in the propagator masses  $m_i^2$  because the zero-frequency modes are excluded from the summation:

$$\begin{aligned}
H_4(m_1, m_2, m_3) &= \int'_{P_1} \int'_{P_2} \int'_{P_3} \delta(P_1 + P_2 + P_3) \\
&\quad \frac{1}{(P_1^2 + m_1^2)(P_2^2 + m_2^2)(P_3^2 + m_3^2)}, \\
L_4(m_1, m_2) &= \int'_{P_1} \int'_{P_2} \frac{(P_1 P_2)^2}{P_1^2(P_1^2 + m_1^2)P_2^2(P_2^2 + m_2^2)}. \quad (13)
\end{aligned}$$

The latter expression cancels algebraically from the sum of the 2-loop contributions. The main properties of the functions  $H_4$  and  $L_4$  appear in Appendix A. The sum of the two-loop contributions without the counterterms, displaying typical three-dimensional linear and logarithmic cut-off dependences leads to the following regularised expression (for the values of the constants  $K_{..}$  and  $I_{..}$ , see Appendix A):

$$V_{\mathcal{E}\mathcal{F}}^{(2)} = \Phi_0^4 \left\{ g^6 \left( \frac{21I_{20}^2}{16} + \frac{15I_3}{64} + \frac{87K_{10}}{128} \right) + g^4 \lambda \left( \frac{33I_{20}^2}{32} - \frac{K_{10}}{64} \right) \right\}$$



$$\begin{aligned}
& +g^2\lambda^2\left(\frac{3I_3}{32}+\frac{K_{10}}{8}\right)+\lambda^3\left(\frac{5I_{20}^2}{18}+\frac{I_3}{24}-\frac{7K_{10}}{108}\right) \\
& +\ln\frac{\Lambda}{T}\left[g^2\lambda^2\frac{K_{1log}}{8}+g^6\left(\frac{87K_{1log}}{128}-\frac{21I_{20}}{128\pi^2}\right)\right. \\
& \left.+g^4\lambda\left(-\frac{K_{1log}}{64}-\frac{33I_{20}}{256\pi^2}\right)+\lambda^3\left(-\frac{7K_{1log}}{108}-\frac{5I_{20}}{144\pi^2}\right)\right] \\
& +\left(\ln\frac{\Lambda}{T}\right)^2\left[-\frac{177g^6}{16384\pi^4}+\frac{9g^4\lambda}{2048\pi^4}-\frac{3g^2\lambda^2}{1024\pi^4}+\frac{\lambda^3}{384\pi^4}\right]\Big\} \\
& +\Phi_0^2\left\{\Lambda^2\left[\lambda^2\left(-\frac{K_{02}}{6}+\frac{I_{20}}{8\pi^2}\right)+g^2\lambda\left(\frac{3K_{02}}{4}+\frac{9I_{20}}{32\pi^2}\right)\right.\right. \\
& \left.+g^4\left(\frac{81K_{02}}{32}+\frac{15I_{20}}{16\pi^2}\right)\right]+\Lambda^2\ln\frac{\Lambda}{T}\left[-\frac{15g^4}{256\pi^4}-\frac{9g^2\lambda}{512\pi^4}-\frac{\lambda^2}{128\pi^4}\right] \\
& +\Lambda T\left[g^4\left(\frac{81K_{01}}{32}-\frac{15I_{20}}{4\pi^2}\right)+g^2\lambda\left(\frac{3K_{01}}{4}-\frac{9I_{20}}{8\pi^2}\right)\right. \\
& \left.+ \lambda^2\left(-\frac{K_{01}}{6}-\frac{I_{20}}{2\pi^2}\right)\right]+\Lambda T\ln\frac{\Lambda}{T}\left[\frac{15g^4}{64\pi^4}+\frac{9g^2\lambda}{128\pi^4}+\frac{\lambda^2}{32\pi^4}\right] \\
& +T^2\left[g^4\left(\frac{5I_{20}}{8}+\frac{81K_{00}}{32}\right)+\lambda g^2\left(\frac{3I_{20}}{16}+\frac{3K_{00}}{4}\right)\right. \\
& \left.+ \lambda^2\left(\frac{I_{20}}{12}-\frac{K_{00}}{6}\right)\right]+T^2\ln\frac{\Lambda}{T}\left[\frac{365g^4}{1024\pi^2}+\frac{27g^2\lambda}{256\pi^2}-\frac{\lambda^2}{32\pi^2}\right]\Big\} \quad (14)
\end{aligned}$$

From this expression beyond the constants, also terms proportional to  $m^2\Phi_0^2$  are omitted. For the required accuracy  $m^2$  can be related on the tree level to the  $T = 0$  Higgs-mass. Since this mass is proportional to  $\lambda$ , the terms proportional to  $m^2$  are actually  $\mathcal{O}(g^4\lambda, g^2\lambda^2, \lambda^3)$ .

One also has to compute the 1-loop non-static counterterm contributions, whose sum is simply:

$$\begin{aligned}
V_{CT} &= \frac{9}{2}m_a^2(Z_{\Phi_1}+2Z_{g_1})I_4(m_a) \\
& +\frac{1}{2}\left(\frac{\lambda}{2}\Phi_0^2(Z_{\lambda_1}+Z_{\Phi_1})+\delta m_1^2\right)I_4(m_a) \\
& +\frac{3}{2}\left(\frac{\lambda}{6}\Phi_0^2(Z_{\lambda_1}+Z_{\Phi_1})+\delta m_1^2\right)I_4(m_a). \quad (15)
\end{aligned}$$

The renormalised potential term of the effective theory can be determined once the wave function renormalisation constants are known, by choosing expressions for  $\delta m^2$  and  $\delta Z_\lambda$  to fulfill some temperature independent renormalisation conditions for the potential energy. So, we need the wave function rescalings to 1-loop accuracy first.

### 3.2 Kinetic terms of the effective theory

The effective kinetic terms are extracted from the gradient expansion of appropriately chosen two-point functions. More closely, they are determined by the coefficients of the linear term in the expansion of the 2-point functions into power series with respect to  $p^2$ . Two kinds of diagrams appear at one-loop level. The tadpole-type is momentum independent. The bubble diagrams are listed in Appendix B accompanied by the corresponding analytic expressions, expanded to  $p^2$  terms.

One adds to the corresponding analytic expressions the "classical value" of the counterterms. The renormalisation constants  $Z$  are fixed by requiring unit residue for the propagators:

$$\begin{aligned} Z_A &= 1 + \frac{25g^2}{48\pi^2}D_0 - \frac{281g^2}{720\pi^2}, \\ Z_\Phi &= 1 + \frac{9g^2}{32\pi^2}D_0 - \frac{g^2}{4\pi^2} \end{aligned} \quad (16)$$

( $D_0 = \ln(\Lambda/T) - \ln 2\pi + \gamma_E$ ). The gauge coupling renormalisation is found by requiring that the gauge mass term proportional to  $\Phi_0^2$ , generated radiatively, vanish (in other words the coupling in front of  $(A_i^a \Phi_0)^2$  stays at  $g^2$ ):

$$Z_g = 1 - \frac{43g^2}{96\pi^2}D_0 + \frac{701g^2}{1440\pi^2} + \frac{\lambda}{48\pi^2}. \quad (17)$$

In terms of the renormalised fields the kinetic term of the effective Lagrangian can be written down by using its invariance under spatial gauge transformations in the usual form:

$$L_{kin} = \frac{1}{4}F_{ij}^a F_{ij}^a + \frac{1}{2}(\nabla_i \Phi)^\dagger \nabla_i \Phi, \quad i, j = 1, 2, 3. \quad (18)$$

### 3.3 Renormalisation

Now, we can write after applying (16) to the  $\Phi_0$ -field that form of the regularised potential energy, where the remaining cut-off dependence of 4-dimensional character is due exclusively to the mass and scalar self-coupling renormalisation:

$$\begin{aligned}
V^{(2)} = & \Phi_0^4 \left\{ \lambda^3 \left( -\frac{19I_{20}^2}{18} + \frac{I_3}{24} - \frac{7K_{10}}{108} \right) + g^4 \lambda \left( -\frac{39I_{20}^2}{32} - \frac{K_{10}}{64} + \frac{3I_{20}}{128\pi^2} \right) \right. \\
& + g^2 \lambda^2 \left( \frac{3I_{20}^2}{2} + \frac{3I_3}{32} + \frac{K_{10}}{8} - \frac{I_{20}}{96\pi^2} \right) \\
& + g^6 \left( \frac{219I_{20}^2}{32} + \frac{15I_3}{64} + \frac{87K_{10}}{128} + \frac{157I_{20}}{2560\pi^2} \right) \\
& + \ln \frac{\Lambda}{T} \left[ g^6 \left( \frac{87K_{1log}}{128} - \frac{157}{40960\pi^4} - \frac{219I_{20}}{256\pi^2} \right) \right. \\
& + g^2 \lambda^2 \left( \frac{K_{1log}}{8} + \frac{1}{1536\pi^4} - \frac{3I_{20}}{16\pi^2} \right) + \lambda^3 \left( -\frac{7K_{1log}}{108} + \frac{19I_{20}}{144\pi^2} \right) \\
& \left. + g^4 \lambda \left( -\frac{K_{1log}}{64} - \frac{3}{2048\pi^4} + \frac{39I_{20}}{256\pi^2} \right) \right] \\
& + \left( \ln \frac{\Lambda}{T} \right)^2 \left[ \frac{177g^6}{16384\pi^4} - \frac{9g^4\lambda}{2048\pi^4} + \frac{3g^2\lambda^2}{1024\pi^4} - \frac{\lambda^3}{384\pi^4} \right] \left. \right\} \\
& + \Phi_0^2 \left\{ \Lambda T \left[ g^4 \left( \frac{81K_{01}}{32} - \frac{157}{2560\pi^4} - \frac{243I_{20}}{32\pi^2} \right) + \lambda^2 \left( -\frac{K_{01}}{6} + \frac{I_{20}}{2\pi^2} \right) \right. \right. \\
& \left. + g^2 \lambda \left( \frac{3K_{01}}{4} - \frac{1}{64\pi^4} - \frac{9I_{20}}{4\pi^2} \right) \right] + \Lambda T \ln \frac{\Lambda}{T} \left[ \frac{243g^4}{512\pi^4} + \frac{9g^2\lambda}{64\pi^4} - \frac{\lambda^2}{32\pi^4} \right] \\
& + \Lambda^2 \left[ \lambda^2 \left( -\frac{K_{02}}{6} - \frac{I_{20}}{4\pi^2} \right) + g^2 \lambda \left( \frac{3K_{02}}{4} + \frac{1}{256\pi^4} + \frac{9I_{20}}{32\pi^2} \right) \right. \\
& \left. + g^4 \left( \frac{81K_{02}}{32} + \frac{157}{10240\pi^4} + \frac{243I_{20}}{128\pi^2} \right) \right] \\
& + \Lambda^2 \ln \frac{\Lambda}{T} \left[ -\frac{243g^4}{2048\pi^4} - \frac{9g^2\lambda}{512\pi^4} + \frac{\lambda^2}{64\pi^4} \right] \\
& \left. + T^2 \left[ \lambda^2 \left( -\frac{I_{20}}{12} - \frac{K_{00}}{6} \right) + g^2 \lambda \left( \frac{3I_{20}}{8} + \frac{3K_{00}}{4} + \frac{1}{384\pi^2} \right) \right] \right\}
\end{aligned}$$

$$\begin{aligned}
& +g^4 \left( \frac{81I_{20}}{64} + \frac{81K_{00}}{32} + \frac{157}{15360\pi^2} \right) \\
& +T^2 \ln \frac{\Lambda}{T} \left[ \frac{81g^4}{256\pi^2} + \frac{3g^2\lambda}{32\pi^2} - \frac{\lambda^2}{48\pi^2} \right] \Bigg\}. \tag{19}
\end{aligned}$$

The final step is to fix the parameters of the renormalised potential energy by enforcing certain renormalisation conditions. We are going to use the simplest conditions, fixing the second and fourth derivatives of the temperature independent part of the potential energy at the origin:

$$\begin{aligned}
\frac{d^2V(T\text{-independent})}{d\Phi_0^2} &= -m^2, \\
\frac{d^4V(T\text{-independent})}{d\Phi_0^4} &= \lambda. \tag{20}
\end{aligned}$$

One pays for this the price of having more complicated relations to the  $T = 0$  physical observables. The connection of the Higgs and of the vector masses as well as the vacuum expectation value of the Higgs field to the couplings renormalised through the above conditions are given in Appendix C.

The renormalised potential term of the reduced model is finally given by

$$\begin{aligned}
V &= \frac{1}{2}m(T)^2\Phi^\dagger\Phi + \frac{\lambda}{24}(\Phi^\dagger\Phi)^2, \\
m(T)^2 &= m^2 + T^2 \left[ \frac{3}{16}g^2 + \frac{1}{12}\lambda + g^4 \left( \frac{81}{32}I_{20} + \frac{81}{16}K_{00} + \frac{157}{7680\pi^2} \right) \right. \\
& \quad \left. + g^2\lambda \left( \frac{3}{4}I_{20} + \frac{3}{2}K_{00} + \frac{1}{192\pi^2} \right) - \lambda^2 \left( \frac{1}{6}I_{20} + \frac{1}{3}K_{00} \right) \right] \\
& \quad + \Lambda T \left[ g^4 \left( \frac{81K_{01}}{32} - \frac{157}{2560\pi^4} - \frac{243I_{20}}{32\pi^2} \right) + \lambda^2 \left( -\frac{K_{01}}{6} + \frac{I_{20}}{2\pi^2} \right) \right. \\
& \quad \left. + g^2\lambda \left( \frac{3K_{01}}{4} - \frac{1}{64\pi^4} - \frac{9I_{20}}{4\pi^2} \right) \right] + \Lambda T \ln \frac{\Lambda}{T} \left[ \frac{243g^4}{512\pi^4} + \frac{9g^2\lambda}{64\pi^4} - \frac{\lambda^2}{32\pi^4} \right] \\
& \quad + T^2 \ln \frac{\Lambda}{T} \left[ \frac{81g^4}{128\pi^2} + \frac{3g^2\lambda}{16\pi^2} - \frac{\lambda^2}{24\pi^2} \right]. \tag{21}
\end{aligned}$$

The last term of (21) can be split into the sum of a finite and an infinite term by introducing a 3d scale  $\mu_3$  into it. It is very remarkable, that the 3d scale dependence at this stage has a coefficient which is of opposite sign relative to what one has in the 3-d SU(2) Higgs model. For the O(N) scalar models this

has been observed by [6]. It cannot be accidental but we did not pursue this phenomenon in the present paper. The scale  $\mu_3$  should not affect the results in the exact solution of the 3d model, but might be tuned at finite order, if necessary.

The finite,  $\mu_3$ -independent piece of the two-loop thermal mass can be parametrized as  $m(T)^2 = k_1 g^4 + k_2 g^2 \lambda + k_3 \lambda^2$  and the numerical values of the coefficients are

$$\begin{aligned} k_1 &= -0.0390912288 \\ k_2 &= -0.0116685842 \\ k_3 &= 0.0027102886. \end{aligned} \tag{22}$$

### 3.4 Non-static nonlocality

The higher terms of the expansion in the external momentum squared ( $\mathbf{p}^2$ ) of the bubble diagrams of Appendix B give rise to non-local interactions of the static fields. For each field a kernel can be introduced, what we shall denote by  $\hat{I}^H(p^2)$ ,  $\hat{I}^G(p^2)$  and  $\hat{I}^A(p^2)$ , respectively. They are defined by subtracting from the full expressions of the corresponding bubbles the first two terms of their gradient expansions, which were taken into account already by the wave function renormalisation and the mass renormalisation locally (see 3.2):

$$\hat{I}^Z(p^2) = I^Z(p^2) - I^Z(0) - p^2 I^{Z'}(0) \tag{23}$$

( $Z = H, G, A$ ). These kernels are used in the calculation of the Higgs-potential from the effective 3-d model at the static 1-loop level (see section 5). Their contribution is of the form of Eq.(89) in Appendix E. In place of the symbol  $m$  in Eq.(89) one should use the mass of the corresponding static field. When working with  $\mathcal{O}(g^4, \lambda g, \lambda^2)$  accuracy, we should use the approximation (95) to the  $\mathbf{p}$ -integral.

Since  $\hat{I}^Z(0) = 0$ , the first term of (95) does not contribute. This is welcome, since this circumstance ensures that no potential linear in  $\Phi_0$  will be produced. Also, we notice that  $\hat{I}^Z(p^2) = \hat{I}_1^Z(p^2)$  (for the notations, see (90)), therefore the integrands of the last terms are given with help of a single function. Nonetheless, as explained in Appendix E, in the second term on the right hand side of (95) one can use the expansion of  $I^Z(p^2)$  with respect to the mass-squares of the non-static fields truncated at linear order, while

in the third term only the mass-independent piece is to be retained. The expression to be used in the first integral we shall denote below by  $\hat{I}^{Z1}$ , while the second by  $\hat{I}^{Z2}$ .

One can point out few useful features of the integrals appearing in (95), allowing the omission of unimportant terms from the full expressions of the kernels. We shall discuss these simplifying remarks first, and present only the relevant pieces from the expressions of the kernels.

There are two kinds of diagrams contributing to each  $\hat{I}^Z$ :

i) the vertices are independent of the background  $\Phi_0$ , and are proportional to  $g$ ,

ii) the vertices are proportional to  $\Phi_0$  and to  $g^2, \lambda$ . In this case the two-point functions actually correspond to certain 4-point vertices, involving two constant external  $\Phi$ -lines. The corresponding non-locality has been discussed for the  $N$ -vector model in [6]. The way we handle them in the present paper seems to us more standardizable.

In case i) the first term of the mass expansion of  $\hat{I}^{Z1}$  is going to contribute to the effective Higgs-potential a constant which will be omitted. On the other hand kernels of this type when multiplied by  $m^2$  in front of the third term of (95) already reach the accuracy limiting our calculation, therefore their mass independent part is sufficient for the computation.

In case ii) the coupling factors in front of each diagram are already  $\mathcal{O}(g^4, \text{etc.})$ , therefore they do not contribute to  $\hat{I}^{Z2}$  in a calculation with the present accuracy, while only their mass independent terms are to be used in  $\hat{I}^{Z1}$ .

Furthermore, some terms of  $\hat{I}^Z(p^2)$  give rise in the calculation of the effective Higgs potential to IR-finite  $\mathbf{p}$ -integrals fully factorised from the rest (this is true in particular for the subtractions from  $I^Z(p^2)$ ). These contributions turn out to be proportional to the UV cut-off and their only role is to cancel against the 3-dimensional "counterterms" generated in the reduction step (see Eq.(21)). We need explicitly only the finite contributions from the integrals. There is no need to present those parts of the kernels which surely do not have any finite contribution.

With these remarks, we restrict ourselves to presenting only the relevant part of the kernels for the three static fields (H,G,A), and also for the static ghost. The occurring integrals as a rule were reduced to unit numerators, with help of the usual "reduction" procedure [11].

The Higgs-nonlocality:

$$\begin{aligned}
\hat{I}^{H1}(p^2) &= \left( -\left(\frac{2}{3}\lambda^2 + \frac{15}{16}g^4\right)\Phi_0^2 + \frac{3g^2m_G^2}{2} - \frac{3g^2m_a^2}{4} \right) \int \frac{1}{K^2(K+p)^2} \\
&\quad + 3g^2p^2 \left( m_G^2 + \frac{1}{2}m_a^2 + \frac{g^2}{8}\Phi_0^2 \right) \int_K \frac{1}{K^4(K+p)^2}, \\
\hat{I}^{H2}(p^2) &= -3g^2p^2 \int_K \left( \frac{1}{2K^2(K+p)^2} - \frac{p^2}{4K^4(K+p)^2} \right). \tag{24}
\end{aligned}$$

The Goldstone-nonlocality:

$$\begin{aligned}
\hat{I}^{G1}(p^2) &= \left( g^2m_G^2 + \frac{1}{2}g^2m_H^2 - \frac{3g^2}{4}m_a^2 - \frac{\lambda^2\Phi_0^2}{9} \right) \int \frac{1}{K^2(K+p)^2} \\
&\quad + 2g^2p^2 \left( \frac{3m_a^2}{4} + \frac{m_H^2}{2} + m_G^2 \right) \int \frac{1}{K^4(K+p)^2}, \\
\hat{I}^{G2}(p^2) &= \frac{3}{2}g^2p^2 \int \left( \frac{1}{K^2(K+p)^2} + \frac{p^2}{2K^4(K+p)^2} \right). \tag{25}
\end{aligned}$$

The magnetic vector nonlocality:

$$\begin{aligned}
\hat{I}^{A1}(p^2) &= 8g^2m_a^2 \int \frac{1}{K^4Q^2} \left[ 4P^2 - 2\frac{(KP)^2}{K^2} - 2\frac{(QP)^2}{Q^2} + \frac{1}{2}(k^2 + q^2 \right. \\
&\quad \left. - \frac{(KP)^2}{P^2} - \frac{(QP)^2}{P^2} \right) \left( 2 + \frac{(KQ)^2}{K^2Q^2} \right) \\
&\quad + \frac{g^2}{2}(3m_G^2 + m_H^2) \int \frac{1}{K^4Q^2} \left( k^2 + q^2 - \frac{(KP)^2}{P^2} - \frac{(QP)^2}{P^2} \right) \\
&\quad + \frac{g^4}{4}\Phi_0^2 \int \frac{1}{K^4Q^2} \left( -2K^2 + k^2 - \frac{(KP)^2}{P^2} \right), \\
\hat{I}^{A2}(p^2) &= -4g^2 \int \frac{1}{K^2Q^2} \left[ 4P^2 - 4\frac{(KP)^2}{K^2} + \left( k^2 - \frac{(KP)^2}{P^2} \right) \left( \frac{(KQ)^2}{K^2Q^2} - 1 \right) \right. \\
&\quad \left. + 3 \left( k^2 - \frac{(KP)^2}{P^2} \right) \frac{K^2 - Q^2}{K^2} \right]. \tag{26}
\end{aligned}$$

The ghost-nonlocality (no ghost contribution arises to the second integral of (95)):

$$\hat{I}^{C1}(p^2) = \frac{1}{2}g^2m_a^2 \int \frac{1}{K^2(K+p)^2} - g^2m_a^2p^2 \int \frac{1}{K^4(K+p)^2}. \tag{27}$$

Two useful remarks can be made concerning the magnetic vector nonlocality:

In the second equation of (26) sometimes only combinations of terms in the integrands prove to be proportional to  $p^2$ . Therefore the corresponding weighted integrals should not be performed term by term.

There are parts of the kernel (26) which could not be reduced to unit numerator, but are proportional to powers of  $\mathbf{k}^2$ . We shall see that upon calculating their contribution to the Higgs effective potential from the 3-d gauge-Higgs effective system, they combine with non-local contributions to the potential from the static  $A_0$  integration (see the end of subsection 4.1 below) into formally Lorentz-invariant contributions.

## 4 Static electric fluctuations

### 4.1 Contribution to the potential term

The  $A_0$ -integration resummed with help of a thermal mass  $m_D$  yields at 1-loop:

$$V^{(1-loop)} = \frac{3}{2} I_3(m_{A0}), \quad (28)$$

defined through the integral

$$I_3(m) = T \int_{\mathbf{k}} \ln(\mathbf{k}^2 + m^2) \quad (29)$$

(its value appears in Appendix A).

At two loops, vacuum diagrams involving one  $A_0$  propagator are listed with their analytic definitions in Appendix D. In addition also three counterterm contributions of (8) should be taken into account on 1-loop level. They can be expressed (up to constant terms) with help of  $I'_3(m_{A0})$  where the prime denotes differentiation with respect to  $m_{A0}^2$ :

$$V_{CT}^{(A0)} = \frac{3T}{2} I'_3(m_{A0}) \left[ -m_D^2 - Z_{A1} m_{A0}^2 + \frac{g^2 \Phi_0^2}{4} (Z_{A1} + Z_{\Phi1} + 2Z_{g1}) \right]. \quad (30)$$

When only terms up to  $\mathcal{O}(g^4)$  are retained and further constants are thrown away, one finds the contribution

$$V_{CT}^{(A0)} = \frac{3T m_D^2 m_{A0}}{8\pi} + \frac{3g^2 T \Phi_0^2 \Lambda}{16\pi^2} (Z_{\Phi1} + 2Z_{g1}). \quad (31)$$



The evaluation of 2-loop diagrams with topology of 'Figure 8' does not pose any problem, since their expressions are automatically factorised into the product of static and nonstatic (sum-)integrals. The evaluation scheme of 'setting sum' diagrams needs, however, some explanation.

Their general form is as appears in (89). Exploiting the analysis of Appendix E we see that the final result of the  $\mathbf{p}$ -integration depends non-analytically on  $m_{A_0}^2$ . The non-analytic piece comes from the first term of the Taylor expansion of the kernel  $I$  with respect to  $\mathbf{p}^2$ :  $I(0) \equiv I'_3(m_{A_0})$ . In other words, this contribution is the product of a static and of a nonstatic integral, similarly to the 'Figure 8' topology. In summary, we find that contributions linear in  $m_{A_0}$  come from the thermal counterterm and from the "factorised" 2-loop expressions. They sum up to

$$\frac{3m_{A_0}}{8\pi} \left( -\frac{5g^2}{2\pi^2} \Lambda T + \frac{5g^2}{6} T^2 - m_D^2 \right). \quad (32)$$

An optimal choice for the resummation mass ( $m_D$ ) is when it is not receiving any finite contribution from higher orders of the perturbation theory. This requirement leads to the equality

$$m_D^2 = \frac{5}{6} g^2 T^2, \quad (33)$$

which means that the two-loop  $A_0$ -contribution at the level of the "local approximation" yields exclusively a linearly diverging, non-polynomial contribution to the potential energy term of the effective 3-d gauge-Higgs model:

$$V_{loc}^{(2-loop)} = \frac{15g^2}{16\pi^3} m_{A_0} \Lambda T. \quad (34)$$

This term plays essential role in the consistent 2-loop perturbative solution of the effective model (see Section 5).

Further terms of the expansion of  $I(p^2)$  are interpreted as higher derivative kinetic terms of  $A_0$ . Their evaluation is based on (95). The only difference relative to the content of subsection 3.4 is that the  $A_0$  integration is performed already at this stage, therefore the contribution from its non-local kinetic action modifies now the potential energy of the Higgs field. When the terms yielding  $\mathcal{O}(g^4, g^2\lambda, \lambda^2)$  accuracy are retained, it turns out that they

actually contribute only to the mass term:

$$\begin{aligned}
& \Phi^\dagger \Phi \left\{ -g^2 \left( \frac{3g^2}{2} + \frac{3}{8}\lambda \right) \int \frac{1}{p^2} \int \frac{1}{Q^4} - \frac{3g^4}{4} \int \frac{1}{p^2} \int \frac{Q_0^2}{Q^6} \right. \\
& + 3g^4 \int \frac{1}{p^2 Q^2 K^4} \left( 2p^2 - \frac{(kp)^2}{K^2} - \frac{(qp)^2}{Q^2} + 2Q_0^2 + Q_0^2 \frac{(KQ)^2}{K^2 Q^2} \right) \\
& + \frac{3}{2}g^2 \left( \lambda + \frac{g^2}{4} \right) \int \frac{Q_0^2}{p^2 Q^2 K^4} - \frac{3}{8}g^4 \int \frac{1}{p^2 Q^2 K^2} \\
& + \frac{3g^4}{2} \int \frac{1}{p^4 Q^2 K^2} \left( 2p^2 - 2\frac{(kp)^2}{K^2} + Q_0^2 \frac{(KQ)^2}{K^2 Q^2} - Q_0^2 \right) \\
& \left. + \frac{9g^4}{2} \int \frac{Q_0^2 (K^2 - Q^2)}{p^4 Q^2 K^4} \right\}. \tag{35}
\end{aligned}$$

In view of the remark at the end of subsection 3.4 on non-static nonlocalities, it is not convenient to evaluate explicitly this contribution already at the present stage. Its Lorentz non-invariant pieces are going to combine in the expression of the final effective Higgs potential with contributions from the static magnetic vector fluctuations into simpler Lorentz invariant integrals (see section 5).

## 4.2 $A_0$ contribution to the gauge-Higgs kinetic terms

The  $A_0$ -bubble contributes to the self-energy of the magnetic vector and of the Higgs (SU(2) singlet) scalar fluctuations. The corresponding analytic expressions are given in Appendix B.

There are two ways to treat these contributions. The first is to apply the gradient expansion again, and retain the finite mass correction and the wave function rescaling factor from the infinite series. This is the approach we followed in case of non-static fluctuations. Then the magnetic vector receives only field rescaling correction:

$$\delta Z_{(A_0)}^A = \frac{g^2 T}{24\pi m_{A_0}}. \tag{36}$$

The Higgs particle receives both finite mass correction and field rescaling factor from the  $A_0$ -bubble:

$$\delta m_{(A_0)}^H = -\frac{3g^4 \Phi_0^2 T}{64\pi m_{A_0}},$$

$$\delta Z_{(A0)}^H = \frac{g^4 \Phi_0^2}{512\pi m_{A0}^3}. \quad (37)$$

One should note that the rescaling factors are  $\mathcal{O}(g)$  what is just the order one has to keep to have the  $\mathcal{O}(g^4)$  accurate effective action [13]. The different behavior of the Higgs and of the Goldstone fields reflects the breakdown of the gauge symmetry in presence of  $\Phi_0$ .

The Higgs-field mass and field rescaling corrections appear only in a non-zero  $\Phi_0$  background. The  $\Phi_0$ -dependence of these quantities will be treated as a non-fluctuating *parametric* effect in the course of solving the effective gauge-Higgs model.

In this case the kernel of the one loop integral is not analytic in  $p^2$ , therefore no basis can be provided for the gradient expansion. Therefore it is important to proceed also the other way, that is to keep the original bubble as a whole in form of a nonlocal part of the effective action. Since its coefficient is  $g^4$ , in the perturbative solution of the effective model it is sufficient to compute its contribution to 1-loop accuracy. (This amounts actually to a two-step evaluation of the of the purely static AAH and AAV setting sun diagrams.)

The difference between the two approaches from the point of view of the quantitative characterisation of the phase transition will be discussed within the perturbative framework in the next Section.

## 5 Two-loop effective Higgs potential from the 3-d effective theory

In this and the next sections we are going to compare various versions of the 3-d theory by calculating perturbatively with their help the characterisation of the electroweak phase transition. This we achieve by finding the respective point of degeneracy of the effective Higgs potential in each approximation. The analysis will be performed for  $g = 2/3$  and  $M_W = 80.6\text{GeV}$ , and for various choices of the  $T = 0$  Higgs mass. (The scheme of the determination of the renormalised parameters is sketched in Appendix C).

## 5.1 Approximations to the effective theory

We start by summarising the effective Lagrangian obtained from the calculations of sections 3 and 4. The parameters were calculated with accuracy  $\mathcal{O}(g^4, \lambda g^2, \lambda^2)$ :

$$\mathcal{L}_{3D} = \frac{1}{4} F_{ij}^a F_{ij}^a + \frac{1}{2} (\nabla_i \Phi)^\dagger (\nabla_i \Phi) + \frac{1}{2} m(T)^2 \Phi^\dagger \Phi + \frac{\lambda_3}{24} (\Phi^\dagger \Phi)^2 - \frac{1}{4\pi} m_{A0}^3 + \mathcal{L}_{nonloc} + \mathcal{L}_{CT}, \quad (38)$$

where

$$\begin{aligned} F_{ij}^a &= \partial_i A_j^a - \partial_j A_i^a + g_3 \epsilon_{abc} A_i^a A_j^b \\ \nabla_i &= \partial_i - i g_3 A_i^a \tau_a, \\ m_{A0}^2 &= g_3^2 \left( \frac{5}{6} T + \frac{1}{4} \Phi^\dagger \Phi \right) \\ m(T)^2 &= m^2 + T^2 \left[ \frac{3}{16} g^2 + \frac{\lambda}{12} + g^4 \left( \frac{81}{32} I_{20} + \frac{81}{16} K_{00} + \frac{157}{7680 \pi^2} \right) \right. \\ &\quad + g^2 \lambda \left( \frac{3}{4} I_{20} + \frac{3}{2} K_{00} + \frac{1}{192 \pi^2} \right) \\ &\quad - \lambda^2 \left( \frac{1}{6} I_{20} + \frac{1}{3} K_{00} \right) + \Delta_{A0}^{nonloc} \\ &\quad \left. + \frac{1}{8\pi^2} \left( \frac{81g^4}{16} + \frac{3g^2\lambda}{2} - \frac{\lambda^2}{3} \right) \ln \frac{\mu_3}{T} \right]. \end{aligned} \quad (39)$$

The dependence of the thermal mass on the 3-d scale is incorrect. The only way to ensure the correct scale dependence of the thermal mass is to include also into the local approximations the effect of the non-static and some of the static nonlocalities.

For this we write down their contribution to the effective Higgs potential combined from (24), (25) (27) on one hand, and from (26) and (35) on the other. The contributions from the different nonlocalities are expressed through some integrals appearing in Appendix A:

*Higgs+Goldstone:*

$$\frac{1}{2} \Phi_0^2 \left[ H_{43}(0, 0, 0) \left( -\lambda^2 - \frac{27}{16} g^4 + 3\lambda g^2 \right) - \frac{d}{dm_1^2} C(0, 0) \left( \frac{15}{8} g^4 + \frac{9}{4} \lambda g^2 \right) \right] \quad (40)$$

*Magnetic and electric vector:*

$$\frac{1}{2}\Phi_0^2 \left[ H_{43}(0, 0, 0) \left( \frac{129}{8}g^4 + \frac{3}{2}\lambda g^2 \right) + \frac{d}{dm_1^2} C(0, 0) \left( \frac{81}{16}g^4 - \frac{3}{4}\lambda g^2 \right) - \frac{3}{2}g^4 \frac{d}{dm_1^2} L_4(0, 0) \right]. \quad (41)$$

*Ghost:*

$$\frac{1}{2}\Phi_0^2 \left[ \frac{3}{4}g^4 H_{43}(0, 0, 0) + \frac{3}{2}g^4 \frac{d}{dm_1^2} C(0, 0) \right]. \quad (42)$$

Using the features of the 3 basic integrals ( $H_{43}, C, L_4$ ), listed in Appendix A, the final numerical expression for the sum of the local (e.g. (22)) plus non-local  $\mathcal{O}(g^4)$  thermal mass terms is the following:

$$\frac{1}{2}\Phi_0^2 \left( 0.0918423g_3^4 + 0.0314655\lambda_3 g_3^2 - 0.0047642\lambda_3^2 + \frac{1}{16\pi^2} \ln \frac{\mu_3}{T} \left( \frac{1}{3}\lambda^2 - \frac{3}{2}\lambda g^2 - \frac{81}{16}g^4 \right) \right). \quad (43)$$

The 2-loop contribution to  $m^2(T)$  could be much influenced by the choice of the 3d renormalisation scale. Through the 4-d renormalisation of the mass-parameter  $m^2$  it is sensitive also to the 4-d normalisation scale (see Appendix C).

All fields in (38) are renormalised 4-d fields multiplied by  $\sqrt{T}$ . The 3-d gauge coupling in the kinetic terms is simply  $g_3 = g\sqrt{T}$ , due to the fact that all finite T-independent corrections are included into  $Z_g$  (cf. eq.(17)). Also the quartic coupling takes the simple form  $\lambda_3 = \lambda T$ , in view of the particular renormalisation condition (20).

The cut-off dependent part of the mass term is hidden in  $\mathcal{L}_{CT}$ . It ensures the cancellation of the cut-off dependence of the 3-d calculations. Except for the non-polynomial term, we are not going to discuss this cancellation. The formal correctness of our effective Higgs potential will be verified by checking its agreement with results of other 3-d calculations, expressed through the parameters  $m^2(T), g_3^2, \lambda_3, m_H^2, m_G^2, m_a^2$ . Off course these parameters themselves are connected to the 4-d couplings differently.

The non-polynomial term of the above Lagrangian is simply the result of the 1-loop  $A_0$ -integration.

Terms of the remaining non-local Lagrangian  $\mathcal{L}_{nonloc}$  are all of the generic form

$$\mathcal{L}_{nonloc} = \frac{1}{2}\phi(-p)\mathcal{N}(p)\phi(p) \quad (44)$$

( $\phi(p)$  refers to general 3-d fields). The kernels  $\mathcal{N}(p)$  are the result of purely static  $A_0$ -loops, listed in Appendix B.

$$\begin{aligned} \mathcal{N}_H(p) &= -\frac{3g_3^4}{8}\Phi_0^2 \int_{\mathbf{k}} \frac{1}{(k^2 + m_{A_0}^2)((k+p)^2 + m_{A_0}^2)} \\ \mathcal{N}_{ij}^a(p) &= -4g^2 \int_{\mathbf{k}} \left[ \frac{k_s \Pi_{si} k_r \Pi_{rj}}{(k^2 + m_{A_0}^2)((k+p)^2 + m_{A_0}^2)} - \frac{1}{3} \frac{k^2 \delta_{ij}}{(k^2 + m_{A_0}^2)^2} \right] \end{aligned} \quad (45)$$

In order to see clearly the effect of the non-polynomial and nonlocal terms we shall consider the effective potential in three different approximations.

*i) Local, polynomial approximation*

In this approximation non-local effects due to the  $A_0$ -bubbles are neglected. The parametric "susceptibilities" of the  $A_i$  and  $\Phi_H$  fields arising from the static  $A_0$ -bubble are included into the approximation (the background  $\Phi_0$  appearing in their expressions is a non-fluctuating parameter!). The non-polynomial term is expanded to fourth power around  $m_D^3$ . In presence of non-zero Higgs background the Lagrangean actually breaks(!) the gauge symmetry (some coefficients explicitly depend on the value of the background field, cf. (37)). The approximate form of the effective Lagrangian is:

$$\begin{aligned} \mathcal{L}_{LP} &= \frac{1}{4\mu} F_{ij}^a F_{ij}^a + \frac{1}{2} (\nabla_i \Phi)^\dagger (\nabla_i \Phi) + \frac{1}{2} Z_H (\partial_i \xi_H)^2 \\ &\quad + V_3(\Phi^\dagger \Phi) + ig_3 \epsilon_{abc} p_i c_a^\dagger(p) A_i^a(q) c_c(k), \end{aligned} \quad (46)$$

with the local potential

$$V_3(\Phi^\dagger \Phi) = \frac{1}{2} (m(T)^2 + \delta m^2) \Phi^\dagger \Phi + \frac{1}{2} \delta m_H^2 \xi_H^2 + \frac{\lambda_3 + \delta \lambda}{24} (\Phi^\dagger \Phi)^2, \quad (47)$$

where

$$\mu = \left(1 + \frac{g_3^2}{24\pi m_{A_0}}\right)^{-1}, \quad \delta \lambda = -\frac{9g_3^4}{64\pi m_D}$$

$$\begin{aligned}\delta m^2 &= -\frac{3g_3^2 m_D}{16\pi}, & \delta m_H^2 &= -\frac{3g_3^4 \Phi_0^2}{64\pi m_{A0}}, \\ Z_H &= \frac{3g_3^4 \Phi_0^2}{512\pi m_{A0}^3},\end{aligned}\tag{48}$$

(the expressions of  $m(T)^2$ ,  $g_3^2$ ,  $\lambda_3$  have been given above). We note, that also a term  $Z_H(A_i^a)^2 \xi_H^2/2$  is present, but it would contribute to higher orders in the couplings, and such terms will not be displayed here.

In order to apply perturbation theory with canonical kinetic terms, one has to rescale both the  $A_i$  and  $\xi_H$  fields:

$$\bar{g}_3 = g_3 \mu^{1/2}, \quad \bar{A}_i = A_i \mu^{-1/2}, \quad \bar{\xi} = \xi_H (1 + Z_H/2).\tag{49}$$

Below we continue to use the *unbarred* notation for these quantities!

After rescalings and the  $\Phi_0$ -shift in the  $R_\alpha$ -gauge the action density is written as

$$\begin{aligned}\mathcal{L}_{LP} &= V_3((1 - Z_H)\Phi_0^2) \\ &+ \frac{1}{2} A_i^a(-k) \left[ (k^2 + m_a^2) \delta_{ij} - (1 - \frac{1}{\alpha}) k_i k_j \right] A_i^a(k) + c_a^\dagger k^2 c_a(k) \\ &+ \frac{1}{2} \xi_H(-k) [k^2 + m_h^2] \xi_H(k) + \frac{1}{2} \xi_a(-k) [k^2 + m_g^2] \xi_a(k) \\ &+ i g_3 S_{abc}^{ijk}(p, q, k) A_i^a(p) A_j^b(q) A_k^c(k) + \frac{1}{8} A_i^2 [g_3^2 \xi_a^2 + g_h^2 \xi_H^2] \\ &+ \frac{g_3^2}{4} [(A_i^a A_i^a)^2 - (A_i^a A_j^a)^2] + \frac{g_h^2 \Phi_0}{4} A_i^2 \xi_H \\ &+ i g_3 \epsilon_{abc} p_i c_a^\dagger(p) A_i^a(q) c_c(k) \\ &- i \frac{1}{2} A_i^a(p) [g_h(k - q)_i \xi_a(q) \xi_H(k) + g_3 \epsilon_{abc} k_i \xi_b(q) \xi_c(k)] \\ &+ \frac{1}{24} (\lambda_{HH} \xi_H^4 + 2\lambda_{HG} \xi_H^2 \xi_G^2 + \lambda_{GG} \xi_a^2) \\ &\Phi_0 \frac{1}{6} \xi_H (q_{HHH} \xi_H^2 + q_{HGG} \xi_a^2) + \mathcal{L}_{CT}^{polym} + \frac{15g^2}{16\pi^3} m_{A0} \Lambda.\end{aligned}\tag{50}$$

Here the expressions for the different couplings read as

$$\begin{aligned}g_h^2 &= g_3^2 (1 - Z_H), & \lambda_{GG} &= \lambda_3 + \delta\lambda \\ \lambda_{HH} &= (\lambda_3 + \delta\lambda)(1 - 2Z_H), & \lambda_{HG} &= (\lambda_3 + \delta\lambda)(1 - Z_H), \\ q_{HHH} &= (\lambda_3 + \delta\lambda)(1 - 2Z_H), & q_{HGG} &= (\lambda_3 + \delta\lambda)(1 - Z_H).\end{aligned}\tag{51}$$

The effective masses of the different fields are

$$\begin{aligned}
m_a^2 &= \frac{g_3^2}{4}\Phi_0^2(1 - Z_H), \\
m_h^2 &= (m(T)^2 + \delta m^2 + \delta m_H^2)(1 - Z_H) + \frac{\lambda_3 + \delta\lambda}{2}\Phi_0^2(1 - 2Z_H), \\
m_g^2 &= m(T)^2 + \delta m^2 + \frac{\lambda_3 + \delta\lambda}{6}\Phi_0^2(1 - Z_H).
\end{aligned} \tag{52}$$

*ii) Local, non-polynomial approximation*

The rescaling and the shift of the fields proceeds as before. The main difference is that here the order of expanding and shifting the  $\Phi$ -field in the non-polynomial term is changed relative to case i). The form of the Lagrangian can be equally written in the form (50). Some expressions and constants appearing in it are modified relative to case i):

$$V_3(\Phi^\dagger\Phi) = \frac{1}{2}(m(T)^2 + \delta m^2)\Phi^\dagger\Phi + \frac{1}{2}\delta m_H^2\xi_H^2 + \frac{\lambda_3 + \delta\lambda}{24}(\Phi^\dagger\Phi)^2 - \frac{1}{4\pi}m_{A0}^3, \tag{53}$$

$$\begin{aligned}
m_{A0}^2 &= m_D^2 + \frac{1}{4}g_h^2\Phi_0^2, \\
\delta m^2 &= -\frac{3g_3^2m_{A0}}{16\pi}, \\
m_h^2 &= (m(T)^2 + \delta m^2 + \delta m_H^2)(1 - Z_H) + \frac{\lambda_3}{2}\Phi_0^2(1 - 2Z_H), \\
m_g^2 &= m(T)^2 + \delta m^2 + \frac{\lambda_3}{6}\Phi_0^2(1 - Z_H),
\end{aligned} \tag{54}$$

$$\begin{aligned}
q_{HGG} &= \lambda_3(1 - Z_H) - \frac{9g_h^2g_3^2}{64\pi m_{A0}}, \\
q_{HHH} &= q_{HGG}(1 - Z_H) + \frac{3g_h^6\Phi_0^2}{256m_{A0}^3}, \\
\lambda_{GG} &= \lambda_3 - \frac{9g_h^4}{64\pi m_{A0}}, \\
\lambda_{HG} &= \lambda_{GG}(1 - Z_H) + \frac{9g_h^4g_3^2\Phi_0^2}{64\pi m_{A0}^3}, \\
\lambda_{HH} &= \lambda_{HG}(1 - Z_H) + \frac{9g_h^6\Phi_0^2}{256\pi m_{A0}^3} - \frac{9g_h^8\Phi_0^4}{1024\pi m_{A0}^5}.
\end{aligned} \tag{55}$$



*iii) Nonlocal, nonpolynomial representation*

Its Lagrangean density coincides with (38), and the major issue of our investigation is the quantitative comparison of its  $\mathcal{O}(g^4)$  solution to the approximate solutions corresponding to cases i) and ii). The couplings  $q_{HHH}$ ,  $q_{HGG}$  and  $\lambda_{HG}$ ,  $\lambda_{GG}$ ,  $\lambda_{HH}$  agree with their expression derived for case ii) when one puts  $Z_H = 0$ ,  $\delta m_H^2 = 0$ .

## 5.2 Variations on the effective Higgs potential

The 1-loop correction to the "classical" value of  $V_3(\Phi_0^2)$  has the unique form for all approximations:

$$V_{eff}^{(1)} = -\frac{1}{12\pi}(6m_a^3 + m_h^3 + 3m_g^3) + \frac{15g_3^2}{16\pi^3}m_{A0}\Lambda + V_{CT}^{polin}(\Phi_0). \quad (56)$$

In this expression cut-off dependent terms with polynomial dependence on  $\Phi_0$  are not displayed, their cancellation is taken for granted. Though the form of this expression is unique, one should keep in mind the variable meaning of the different masses from one approximation to the other. From the point of view of consistent cancellation of non-polynomial divergences it is important to notice, that the 1-loop linear divergences of the Higgs- and Goldstone-fields by the contribution of the shifted non-polynomial term to their respective mass produce a non-polynomial cut-off dependent term  $(-3g_3^2/16\pi^3)\Lambda m_{A0}$  (in cases ii) and iii) only) to be compared with the induced non-polynomial divergence eq.(34). In the first two approximation schemes no further divergences of this form are produced, therefore their cut-off dependence is clearly different from what is generated in the course of the integration. Below, for cases i) and ii) we assume the presence of the appropriately modified counterterms.

The 2-loop diagrams of a local, 3-d gauge-Higgs system are the same as in 4-d. Just the functions appearing in the expressions are defined as three-dimensional momentum integrals. In purely algebraic steps one can work out the general representation given in terms of the functions  $I_3(m^2)$ ,  $H_3(m_1, m_2, m_3)$  (see Appendix A), to arrive finally at the following 2-loop contribution:

$$V_{eff}^{(2)} = L_0 \left( \frac{63g^2 m_a^2}{8} - \frac{3g_h^2 m_a^2}{2} + \frac{3g^2 m_G^2}{2} + \frac{3g_h^2 m_G^2}{4} + \frac{3g^2 m_H^2}{4} - \frac{q_{GGH}^2 + q_{HHH}^2}{12} \Phi_0^2 \right) + \frac{1}{128\pi^2} (5\lambda_{GG} m_G^2 + 2\lambda_{GH} m_G m_H + \lambda_{HH} m_H^2)$$

$$\begin{aligned}
& + \frac{g^2}{128\pi^2} \left( (9 - 63 \ln 3) m_a^2 - \frac{3g_h^2 m_a^2}{g^2} + 12m_a m_G - \frac{3g_h^2 m_a m_G}{g^2} \right. \\
& \left. \frac{6g_h^2 m_a m_H}{g^2} + 3m_G^2 + \frac{3g_h^2 m_G m_H}{g^2} + \frac{3g_h^2 m_H^2}{2g^2} \right) \\
& - \frac{3g_h^2}{128\pi^2} \frac{m_H - m_G}{m_a} (m_H^2 - m_G^2) \\
& + \frac{q_{GGH}^2 \Phi_0^2}{192\pi^2} \ln \frac{2m_G + m_H}{T} + \frac{q_{HHH}^2 \Phi_0^2}{192\pi^2} \ln \frac{3m_H}{T} \\
& + \frac{3}{64\pi^2} \left[ g_h^2 m_H^2 \ln \frac{m_a + m_H}{2m_a + m_H} + \frac{g_h^2 m_H^4}{4m_a^2} \ln \frac{m_H(2m_a + m_H)}{(m_a + m_H)^2} \right. \\
& \left. + \frac{g_h^2 (m_H^2 - m_G^2)^2}{2m_a^2} \ln \frac{m_a + m_G + m_H}{m_G + m_H} \right. \\
& \left. - g_h^2 \left( m_H^2 + m_G^2 - \frac{m_a^2}{2} \right) \ln \frac{m_a + m_G + m_H}{T} \right. \\
& \left. + g^2 \left( \frac{m_a^2}{2} - 2m_G^2 \right) \ln \frac{m_a + 2m_G}{T} - \frac{g_h^2 m_a^2}{2} \ln \frac{m_a + m_H}{T} \right. \\
& \left. + 2g_h^2 m_a^2 \ln \frac{2m_a + m_H}{T} - 11m_a^2 \ln \frac{m_a}{T} \right]. \tag{57}
\end{aligned}$$

The final step of composing the full effective potential corresponds to picking up the contributions of the purely static **VAA**, and **HAA** diagrams:

$$\begin{aligned}
V_{eff}^{(2nonloc)} & = 6g_3^2 L_0(m_{A0}^2 - \frac{3}{8}m_a^2) + \frac{3g_3^2}{32\pi^2} (m_{A0}^2 + 2m_{A0}m_a) - \frac{12g_3^2}{16\pi^3} \Lambda m_{A0} \\
& - \frac{3g_3^2}{32\pi^2} [(4m_{A0}^2 - m_a^2) \ln \frac{2m_{A0} + m_a}{\mu_3} \\
& - \frac{1}{2}m_a^2 \ln \frac{2m_{A0} + m_H}{\mu_3}]. \tag{58}
\end{aligned}$$

The cancellation of the linear divergence, nonpolynomial in  $\Phi_0^2$  can be seen explicitly.

The 2-loop corrections to the effective potential, given by Eqs.(57) and (58) can be compared to the results of the direct 4-d calculation of [12, 14]. Those calculations were done with different regularisation and renormalisation scheme, therefore in the expression of the potential terms reflecting this difference are seen. Still, using the leading expressions for our couplings

$g_h, q_{GGH}, q_{HHH}, \lambda_{GG}, \lambda_{GH}$  and  $\lambda_{HH}$ , all logarithmic terms expressed through the propagator masses agree. Also our polynomial terms, except those proportional to the regularisation dependent coefficient  $L_0$ , have their exact counterpart in the 4-d expression. The  $T$ -independent contribution appearing in the 4d result has no corresponding term in our case, an obvious effect of the difference of the renormalisation schemes. The polynomial terms explicitly depending on  $\bar{\mu}$  and proportional to the constants  $c_1, c_2$  characteristic for the dimensional regularisation, can be compared to our terms proportional to  $L_0$ . Choosing in both potentials  $\mu = T$ , one finds in the 4-d expression for the coefficients of the terms  $g^2 m_W^2, g^2(m_H^2 + 3m_G^2)$  and  $\lambda^2 \Phi_0^2$ , the values  $2.441 \times 10^{-2}, 4.012 \times 10^{-3}, -2.239 \times 10^{-4}$ , respectively. The corresponding coefficients from our expression are:  $2.765 \times 10^{-2}, 5.027 \times 10^{-3}, -5.374 \times 10^{-4}$ . Therefore the only origin of considerable deviations in physical quantities could be the effect of the reduction on various couplings. Our numerical experience was that the  $\mathcal{O}(g^4)T^2$  correction in  $m^2(T)$  accounts for essentially all differences.

## 6 Phase transition characteristics

In this section we describe and discuss the phase transition in the three perturbative approximations introduced in the previous section. Our analysis will cover the Higgs mass range 30 to 120 GeV. Our main interest lies in finding the percentual variation in the following physical quantities: the critical temperature ( $T_c$ ), the Higgs discontinuity ( $\Phi_c$ ), the surface tension ( $\sigma$ ) and the latent heat ( $L_c$ ). The amount of variation from one approximation to the other will give an idea of the theoretical error coming from the reduction step.

The first step of the calculation consists to choose values for  $g$  and  $\lambda$ . For example one can fix  $g = 2/3$  and tune  $\lambda$  guided by the tree-level Higgs-to-gauge boson mass ratio. All dimensional quantities are scaled by appropriate powers of  $|m|$  (what practically amounts to set  $|m| = 1$  in the expressions of the Higgs effective potential).

Next, one finds from the degeneracy condition of the effective potential the ratio  $T_c/|m|$ . Here we have to discuss a phenomenon already noticed by [12]. It has been observed that for Higgs mass values  $m_H \geq 100\text{GeV}$  when the temperature is lowered one reaches the barrier temperature before the dege-

naracy of the minima would occur. The phenomenon was traced back to the action of the term  $\sim g^2 m_{A_0}(m_H + 3m_G)$  in the effective potential. In our non-polynomial approximation the  $A_0$ -integration contributes a negative term to  $m^2(T)$  (i.e.  $\delta m^2$ ), which acts even stronger, and the same phenomenon is generated, when using  $\mu_3 = T$ , already for  $m_H \leq 70\text{GeV}$ . However, by choosing somewhat more exotic value for the normalisation scale ( $\mu_3 = T/17$ ), we could follow the transition up to  $m_H = 120\text{GeV}$ . We have used this value in the whole temperature range. It has been checked for  $m_H = 35\text{GeV}$  that the variation of  $\mu_3$  leads in the physical quantities to negligible changes.

Finally, the relations of Appendix C allow to express with  $\mathcal{O}(g^4)$  accuracy the ratios  $M_W/|m|$  and  $M_H/|m|$  with help of  $g, \lambda$  and  $T_c/|m|$  (the dependence on the latter appears through our choice of the 4-d normalisation point). The pole mass  $M_H$  resulting from this calculation appears in column 2 of Table 1, where  $M_W = 80.6\text{GeV}$  sets the scale in physical units. Our 4-d renormalisation scheme leads to somewhat smaller mass shifts, than the scheme used in [15].

In order to present physically meaningful plots one has to eliminate from these relations  $|m|$  and scale everything by an appropriate physical quantity. In Fig. 1 (column 3 of Table 1) we present  $T_c/M_H$  as a function of  $M_H/M_W$  in the non-polynomial non-local (NNA) approximation (upper case notation for the masses always refer to  $T=0$  pole mass). Internally, our different approximations do not affect the critical temperature, they all agree within better than 1%, as can be seen in Table 2. The curve in Fig.1 is, however, systematically below the data appearing in Table 2 of [15]. 15% deviation is observed for  $m_H = 35\text{GeV}$ , which gradually decreases to 8% for  $m_H = 90\text{GeV}$ . If one wishes to compare to the 2-loop 4d calculations of [12, 14] one has to use their coupling point:  $g = 0.63722, m_W = 80.22$ . Again we find that our  $T_c/m_H$  values are 10% lower than those appearing in Fig.4 of [14]. Our  $\mathcal{O}(g^4)T^2$  correction to  $m^2(T)$  is about 10% of the 1-loop value (and is about 9 times larger than what was found in [15]), therefore one qualitatively understands that the barrier temperature is brought down in about the same proportion. At least in the region  $M_W \simeq M_H$  the transition is already so weak that the transition temperature should agree very well with the temperatures limiting the metastability range.

In Fig. 2 (column 4 of Table 1) the order parameter discontinuity is displayed in proportion to  $T_c$ . Here the agreement is extremely good in the whole 35-90 GeV range both in comparison to [15, 9] and [14]. Also the

variance of our different approximations (see Table 2) is minimal.

The most interesting is the case of the surface tension, which is shown for all three approximations in Fig.4 in  $(GeV)^4$  units (the dimensionless ratio appears in column 5 of Table 1). We did not observe any strengthening tendency for larger Higgs masses, in contrast to [12]. This systematic difference seems to be correlated with the extended range where we find phase transition. It leads to  $\sigma_c$  values in the range  $M_H = 50 - 80 GeV$  which perfectly agree with the perturbative values quoted by [9]. The dispersion between the values of our different approximations is much larger in the high mass range (Table 2) than for other quantities, reflecting the increased sensitivity to non-local and non-polynomial contributions.

The situation is just a little less satisfactory in case of the latent heat (Fig.3 and column 6 of Table 1). Our approximations are 10-15% above  $L_c/T_c^4$  curve of Fig.6 of [14] and also of the perturbative values in Table 6 of [9].

## 7 Conclusions

In this paper we have attempted to discuss in great detail the reduction strategy, allowing non-renormalisable and non-local effective interactions. We have made explicit the effect of various approximations on the phase transition characteristics of the SU(2) Higgs model. Our investigation remained within the framework of the perturbation theory. By comparing with other perturbative studies [12, 14, 15] we have pointed out that the  $T_c/M_H$  ratio is quite sensitive to the choice of the 3-d renormalisation scale. The order parameter discontinuity and the the surface tension were found only moderately sensitive, while the latent heat in the  $\overline{MS}$  scheme seems to drop faster with increasing Higgs mass. The minimum of the surface tension when  $M_H$  is varied has disappeared. One might wonder to what extent is the strengthening effect observed in the 4-d perturbative treatment with increasing Higgs mass physical at all.

The local polynomial and the local non-polynomial approximations start to show important (larger than 5%) deviations from the nonlocal, nonpolynomial version of the effective model only for  $M_H \geq 80 GeV$  (also below 30GeV). Since in these regions the perturbation theory becomes anyhow unreliable, we can say that the application of the reduction to the description of the

electroweak phase transition in the relevant Higgs mass range ( $M_H \sim M_W$ ) could be as accurate as 5%. This can be true for dimensionless ratios, but not for  $T_c/M_H$ .

The present assessment of the accuracy is not universal, though the structure of the analysis is quite well fitting other field theoretic models, too. For instance, our methods could be applied to extended versions of the electroweak theory [17, 18, 19] which are accessible to quantitative non-perturbative investigations only in 3-d reduced form.

One knows that non-perturbative studies of the SU(2) Higgs transition led to lower  $T_c/M_H$  ratio, than the perturbative prediction [20], and at least for  $M_H = 80\text{GeV}$  the surface tension is much lower than it was thought on the basis of the strenghtening effect [21]. The results from the PPI-reduction seems to push the perturbative phase transition characteristics towards this direction. The expressions of the mass parameter of the effective theory (21) and the T=0 pole masses (Appendix C) provide the necessary background for the analysis of 3-d non-perturbative investigations following the strategy advocated by [16, 9]. This will be the subject of a forthcoming publication [22].

## A Important integrals

All integrals have been performed with 3-d momentum cut-off  $\Lambda$ . The capital subscript denotes finite temperature sum-integral, the bold lower case index refers to 3-d momentum space integration. The prime on the sum-integral means summation over the non-static modes only.

1.

$$\begin{aligned}
I_4(m) &= I_0 + I_1 m^2 + I_2 m^4 + \dots \\
I_1 &= \frac{\Lambda^2}{8\pi^2} - \frac{\Lambda T}{2\pi^2} + \frac{T^2}{12} \\
&\equiv I_{12}\Lambda^2 + I_{11}\Lambda T + I_{10}T^2 \\
I_2 &= -\frac{1}{16\pi^2} \ln \frac{\Lambda}{T} + \frac{1}{16\pi^2} (1 + \ln(2\pi) - \gamma_E) \\
&\equiv I_{2ln} \ln \frac{\Lambda}{T} + I_{20}.
\end{aligned} \tag{59}$$

2.

$$\begin{aligned}
I_3(m) &= \frac{1}{2\pi^2}\Lambda m^2 - \frac{1}{6\pi}m^3 \\
&\equiv 2J_1\Lambda m^2 + 2J_0m^3.
\end{aligned} \tag{60}$$

3.

$$\begin{aligned}
H_4(m_1, m_2, m_3) &= K_0 + K_1 \frac{m_1^2 + m_2^2 + m_3^2}{3} + \dots \\
K_0 &= 0.0001041333\Lambda^2 - 0.0029850437\Lambda T + \frac{5}{32\pi^2}T^2 \ln \frac{\Lambda}{T} \\
&\quad - 0.0152887686T^2 \\
&\equiv K_{02}\Lambda^2 + K_{01}\Lambda T + K_{0ln} \ln \frac{\Lambda}{T} + K_{00}T^2 \\
K_1 &= -\frac{3}{128\pi^4}(\ln \frac{\Lambda}{T})^2 + 0.001087871 \ln \frac{\Lambda}{T} + \text{const.} \\
&\equiv K_{10}(\ln \frac{\Lambda}{T})^2 + K_{1log} \ln \frac{\Lambda}{T} + \text{const..}
\end{aligned} \tag{61}$$

4.

$$\begin{aligned}
H_3(m_1, m_2, m_3) &= \frac{1}{32\pi^2} \ln \frac{\Lambda^2}{(m_1 + m_2 + m_3)^2} + L_0, \\
L_0 &= 6.70322 \times 10^{-3}.
\end{aligned} \tag{62}$$

5.

$$\begin{aligned}
H_{43} &= \int'_{P_1} \int'_{P_2} \int_{\mathbf{P}} \frac{1}{(P_1^2 + m_1^2)(P_2^2 + m_2^2)(\mathbf{P}^2 + m_3^2)} \\
&= a_1\Lambda T - \frac{1}{16\pi^2}T^2 \ln \frac{\Lambda}{T} + a_2T^2 + \frac{m_3T}{32\pi^3}(\ln \frac{\Lambda}{T} - 16\pi^2 I_{20}) \\
&\quad + a_3m_3^2 - \frac{1}{768\pi^2}(m_1^2 + m_2^2) + \dots,
\end{aligned} \tag{63}$$

$$a_1 = 0.000995014555, \quad a_2 = 0.0074744795, \quad a_3 = 0.0000659642. \tag{64}$$

6.

$$\begin{aligned}
L_4(m_1, m_2) &= \int'_{P_1} \int'_{P_2} \frac{(P_1 P_2)^2}{P_1^2(P_1^2 + m_1^2)P_2^2(P_2^2 + m_2^2)} \\
&= L_{40} + \left[ \frac{T^2}{768\pi^2} - \right. \\
&\quad \left. - \frac{\Lambda T}{128\pi^4} \left( \ln \frac{\Lambda}{T} - (1 + \ln(2\pi) - \gamma_E) \right) \right] (m_1^2 + m_2^2). \quad (65)
\end{aligned}$$

7.

$$\begin{aligned}
C(m_1, m_2) &= T^2 \sum_{n \neq 0} \int_{\mathbf{k}} \int_{\mathbf{q}} \frac{1}{(\omega_n^2 + \mathbf{k}^2 + m_1^2)} \frac{1}{(\omega_n^2 + \mathbf{q}^2 + m_2^2)} \\
&= C_0 + (m_1^2 + m_2^2)C_1 + \dots, \quad (66)
\end{aligned}$$

$$C_1 = -\frac{1}{16\pi^4} \Lambda T \left( \log \frac{\Lambda}{T} - 1 - \ln(2\pi) + \gamma_E \right) - \frac{T^2}{32\pi^2}. \quad (67)$$

## B Momentum dependent (bubble) contributions to 2-point functions

In this Appendix we give a list of the diagrams generating higher momentum-dependent vertices of the reduced theory. Each bubble contains two internal lines, which we use for "naming" the diagrams. (The abbreviations are: V – for non-static magnetic vector potential, H – for non-static Higgs, G – for non-static Goldstone, C – for non-static ghost and A – for static electric potential). Some diagrams are proportional also to  $\Phi_0^2$ , so they actually correspond to 4-point functions. The 2-point approach is just a convenient way to study their momentum dependence. All 2-point functions depend on the spatial momentum  $K = (0, \mathbf{k})$ . The first few terms of the gradient expansion of each diagram will be given up to that term which should be considered in the evaluation of local mass and wave function renormalisations. These terms are subtracted from the full expression, when one turns to the investigation of non-local effects (see Appendix E).

*Higgs 2-point function*



$$\begin{aligned}
\frac{g^2}{8} \mathbf{V} \mathbf{G} &= -3g^2 \int_P \left( k^2 - \frac{(KP)^2}{P^2} \right) \frac{1}{P^2 + m_a^2} \frac{1}{(P+k)^2 + m_G^2} \\
&\simeq -g^2 k^2 \int_P \left[ 3 - \frac{p^2}{P^2} \right] \frac{1}{P^2 + m_a^2} \frac{1}{P^2 + m_G^2}
\end{aligned} \tag{68}$$

$$\begin{aligned}
-\frac{g^4}{32} \Phi_0^2 \mathbf{V} \mathbf{V} &= -\frac{3g^4 \Phi_0^2}{8} \int_P \frac{1}{P^2 + m_a^2} \frac{1}{(P+k)^2 + m_a^2} \left( 2 + \frac{(P(P+k))^2}{P^2(P+k)^2} \right) \\
&\simeq -\frac{9g^4 \Phi_0^2}{8} \int_P \frac{1}{(P^2 + m_a^2)^2},
\end{aligned} \tag{69}$$

$$\begin{aligned}
-\frac{\lambda^2}{72} \Phi_0^2 \mathbf{H} \mathbf{H} &= -\frac{\lambda^2 \Phi_0^2}{2} \int_P \frac{1}{P^2 + m_H^2} \frac{1}{(P+k)^2 + m_H^2} \\
&\simeq -\frac{\lambda^2 \Phi_0^2}{2} \int_P \frac{1}{(P^2 + m_H^2)^2},
\end{aligned} \tag{70}$$

$$\begin{aligned}
-\frac{\lambda^2}{72} \Phi_0^2 \mathbf{G} \mathbf{G} &= -\frac{\lambda^2 \Phi_0^2}{6} \int_P \frac{1}{P^2 + m_G^2} \frac{1}{(P+k)^2 + m_G^2} \\
&\simeq -\frac{\lambda^2 \Phi_0^2}{6} \int_P \frac{1}{(P^2 + m_G^2)^2},
\end{aligned} \tag{71}$$

$$-\frac{g^4}{32} \Phi_0^2 \mathbf{A} \mathbf{A} = -\frac{3g^4 \Phi_0^2}{8} \int_{\mathbf{p}} \frac{1}{p^2 + m_{A0}^2} \frac{1}{(p+k)^2 + m_{A0}^2}. \tag{72}$$

This last integral is not analytic in  $k^2$ , therefore its gradient expansion is a dangerous step.

*Goldstone 2-point function*

$$\begin{aligned}
\frac{g^2}{8} \mathbf{V} \mathbf{G} &= -2g^2 \int_P \left( k^2 - \frac{(KP)^2}{P^2} \right) \frac{1}{P^2 + m_a^2} \frac{1}{(P+k)^2 + m_G^2} \\
&\simeq -2g^2 k^2 \int_P \left[ 1 - \frac{p^2}{3P^2} \right] \frac{1}{P^2 + m_a^2} \frac{1}{P^2 + m_G^2},
\end{aligned} \tag{73}$$

$$\begin{aligned}
\frac{g^2}{8}\mathbf{VH} &= -g^2 \int_P \left(k^2 - \frac{(KP)^2}{P^2}\right) \frac{1}{P^2 + m_a^2} \frac{1}{(P+k)^2 + m_H^2} \\
&\simeq -g^2 k^2 \int_P \left[1 - \frac{p^2}{3P^2}\right] \frac{1}{P^2 + m_a^2} \frac{1}{P^2 + m_H^2}, \tag{74}
\end{aligned}$$

$$\begin{aligned}
-\frac{\lambda^2}{72}\Phi_0^2\mathbf{HG} &= -\frac{\lambda^2\Phi_0^2}{9} \int_P \frac{1}{P^2 + m_H^2} \frac{1}{(P+k)^2 + m_G^2} \\
&\simeq -\frac{\lambda^2\Phi_0^2}{9} \int_P \frac{1}{P^2 + m_H^2} \frac{1}{P^2 + m_G^2}. \tag{75}
\end{aligned}$$

*Magnetic vector 2-point function*

Here we give the contributions to the polarisation tensor  $\mathcal{N}_{ij}$ . When the static  $A_i$  legs are contracted, its contribution to the effective Higgs potential is of the form (see Appendix E):

$$\int \frac{\mathcal{N}_{ij}(p)\Pi_{ij}}{p^2} - m_a^2 \int \frac{(\mathcal{N}_{ij}(p) - \mathcal{N}_{ij}(0))\Pi_{ij}}{p^4}, \tag{76}$$

where  $\Pi_{ij} = \delta_{ij} - p_i p_j / p^2$ . The following bubbles contribute:

$$\begin{aligned}
\frac{g^2}{2}\mathbf{VV} &= -4g^2 \int \frac{1}{(K^2 + m_a^2)(Q^2 + m_a^2)} \left[ 2\Pi_{ij} \left( p^2 - \frac{(pK)^2}{K^2} \right) \right. \\
&\quad \left. + K\Pi_i K\Pi_j \left( 3 + 2\frac{pK}{K^2} + \frac{(Kp)(Qp)}{K^2 Q^2} \right) \right] \\
&\simeq -4g^2 \Pi_{ij} \int \frac{k^2}{(K^2 + m_a^2)^2} - 4g^2 p^2 \Pi_{ij} \left[ 2 \int \frac{1}{(K^2 + m_a^2)^2} \right. \\
&\quad - \frac{2}{3} \int \frac{k^2}{K^2(K^2 + m_a^2)^2} - \int \frac{k^2}{(K^2 + m_a^2)^3} \\
&\quad + \frac{4}{5} \int \frac{k^4}{(K^2 + m_a^2)^4} - \frac{4}{15} \int \frac{k^4}{K^2(K^2 + m_a^2)^3} \\
&\quad \left. - \frac{1}{15} \int \frac{k^4}{K^4(K^2 + m_a^2)^2} \right] \\
\frac{g^2}{8}\mathbf{GH} &= -g^2 \int \frac{K\Pi_i K\Pi_j}{(K^2 + m_H^2)(Q^2 + m_G^2)}
\end{aligned}$$

$$\begin{aligned}
& \simeq -\frac{g^2}{3}\Pi_{ij} \int \frac{q^2}{(Q^2 + m_H^2)(Q^2 + m_G^2)} \\
& \quad + \frac{g^2}{3}p^2\Pi_{ij} \left[ \int \frac{q^2}{(Q^2 + m_H^2)(Q^2 + m_G^2)^2} \left( 1 - \frac{4}{5} \frac{q^2}{Q^2 + m_G^2} \right) \right] \\
\frac{g^2}{8}\mathbf{GG} &= -g^2 \int \frac{K\Pi_i K\Pi_j}{(K^2 + m_G^2)(Q^2 + m_G^2)} \\
& \simeq -\frac{g^2}{3}\Pi_{ij} \int \frac{k^2}{(K^2 + m_G^2)^2} \\
& \quad + \frac{g^2}{3}p^2\Pi_{ij} \left[ \int \frac{k^2}{(K^2 + m_G^2)^3} \left( 1 - \frac{4}{5} \frac{k^2}{K^2 + m_G^2} \right) \right] \\
-\frac{g^4}{32}\Phi_0^2\mathbf{VH} &= -\frac{g^4}{4}\Phi_0^2 \int \frac{1}{(K^2 + m_a^2)(Q^2 + m_H^2)} \left[ \Pi_{ij} - \frac{K\Pi_i K\Pi_j}{K^2} \right] \\
& \simeq -\frac{g^4}{4}\Phi_0^2\Pi_{ij} \int \frac{1}{(K^2 + m_H^2)(K^2 + m_a^2)} \left( 1 - \frac{1}{3} \frac{k^2}{K^2} \right) \\
\frac{g^2}{2}\mathbf{CC} &= 2g^2 \int \frac{K\Pi_i K\Pi_j}{K^2 Q^2} \\
& \simeq \frac{2g^2}{3}\Pi_{ij} \int \frac{k^2}{K^4} - \frac{2g^2}{3}p^2\Pi_{ij} \int \frac{k^2}{K^6} \left( 1 - \frac{4}{5} \frac{k^2}{K^2} \right) \\
\frac{g^2}{2}\mathbf{AA} &\simeq -\frac{4}{3}g^2 \int \frac{k^2}{(k^2 + m_{A0}^2)^2} \left[ 1 - \frac{p^2}{k^2 + m_{A0}^2} + \frac{4}{5} \frac{p^2 k^2}{(k^2 + m_{A0}^2)^2} \right] \quad (77)
\end{aligned}$$

$(K\Pi_i \equiv k_j(\delta_{ij} - p_i p_j/p^2))$ .

*Ghost 2-point function*

$$\frac{g^2}{2}\mathbf{CV} = 2g^2 \int_K \left( p^2 - \frac{(PK)^2}{K^2} \right) \frac{1}{K^2 + m_a^2} \frac{1}{(P+K)^2} \quad (78)$$

## C Couplings in terms of $T = 0$ physical quantities

At tree level the renormalised couplings and the vacuum expectation value of the Higgs-field ( $v$ ) determine the masses of the field quanta:

$$m_H^2 = m^2 + \frac{\lambda}{2}v^2,$$

$$m_W^2 = \frac{g^2}{4}v^2. \quad (79)$$

Physical masses are approximated by finding the roots at  $\mathbf{p}^2 = -m^2$  of the corresponding 2-point functions. For achieving the accuracy  $\mathcal{O}(g^4, \dots)$  we need also the vacuum expectation value  $v$  corrected by 1-loop fluctuations. For this we calculate the minimum of the  $T = 0$  renormalised effective Higgs potential to 1-loop from the condition:

$$\begin{aligned} \frac{dV_{eff}(v)}{dv^2} &= \frac{1}{2}m^2(1 - 2\lambda I_{20}) + \frac{1}{12}\lambda v^2(1 - \frac{27g^4}{4\lambda}I_{20} - 4\lambda I_{20}) \\ &+ \frac{1}{64\pi^2} \left( \frac{9g^2}{2}m_W^2 \ln \frac{m_W^2}{T^2} + \lambda m_G^2 \ln \frac{m_G^2}{T^2} + \lambda m_H^2 \ln \frac{m_H^2}{T^2} \right) \\ &= 0. \end{aligned} \quad (80)$$

For the accuracy requested it is sufficient to use in the 1-loop part the tree level expressions (79). Then the iterative solution is easily found:

$$\begin{aligned} v^2 &= -\frac{6m^2}{\lambda} \left( 1 + \left( 2\lambda + \frac{27g^4}{4\lambda} \right) I_{20} \right. \\ &\left. - \frac{1}{64\pi^2} \left[ \frac{27g^4}{2\lambda} \ln \left( \frac{3g^2}{2\lambda} \left( -\frac{m^2}{T^2} \right) \right) + 4\lambda \ln \left( -\frac{2m^2}{T^2} \right) \right] \right). \end{aligned} \quad (81)$$

For the Higgs and W-masses one makes use of their 2-point functions. Here again we use  $\mu = T$  and neglect the running of the couplings to the scale where they are usually measured (say at  $m_W$ ). (This should be used only in the tree level mass expressions, if necessary.)

The 4-d integrals were evaluated with cut-off regularisation. We have reduced all the 1-loop integrals to 1-variable integrals with help of Feynman parametrisation. For a set of numerical values of  $g, \lambda$  one finds  $M_H^2$  and  $M_W^2$ , the 1-loop accurate masses in proportion to the renormalised mass parameter  $-m^2$  to be still functions of the logarithms of  $m_H^2/T^2$  and of  $m_W^2/T^2$ . In the arguments of the logarithms the tree level mass expressions can be used. This leads to the unique dependence on  $-m^2/T^2$ . The numerical value of the latter for fixed values of  $g, \lambda$  is extracted from the degeneracy condition imposed on the minima of the effective potential (see section 6). Having the value of  $\ln(-m^2/T^2)$ , the integrations over the Feynman parameter can be done.

Below we give the expressions of the 1-loop accurate Higgs and W-masses before the 1-dimensional integrals are performed.

The 1-loop accurate expression of the Higgs-mass is

$$M_H^2 = m_H^2 + \Sigma(-m_H^2). \quad (82)$$

The self-energy of the Higgs field is given by

$$\begin{aligned} \Sigma(-m_H^2) &= -\frac{3g^2 m_W^2}{64\pi^2} (9 - 3h^2 + \frac{1}{2}h^4) \ln \frac{T^2}{m_W^2} - \frac{\lambda m_H^2}{8\pi^2} \ln \frac{T^2}{m_H^2} \\ &\quad + \frac{\lambda m_H^2}{32\pi^2} (\pi\sqrt{3} - \frac{89}{30}) + \frac{3g^2 m_W^2}{32\pi^2} \left( 3 - \frac{7h^2}{12} + \frac{h^4}{8} - Q_H(h^2) \right) \\ &\quad + \Sigma_{CT}(-m_H^2), \end{aligned} \quad (83)$$

where  $h \equiv m_H/m_W$  and the one-variable integral  $Q_H$  is defined as

$$\begin{aligned} Q_H(h^2) &= \int_0^1 dx \left[ 1 + h^2 \left( \frac{1}{2} - 12x + 12x^2 \right) + h^4 x \left( -\frac{1}{2} + \frac{21}{2}x - 20x^2 + 10x^3 \right) \right] \\ &\quad \times \ln(1 - h^2 x(1 - x)). \end{aligned} \quad (84)$$

The contribution coming from the 1-loop counterterms is

$$\Sigma_{CT} = \frac{m_H^2}{16\pi^2} (1 + \ln(2\pi) - \gamma_E) \left( \frac{9g^2}{2} - 4\lambda - \frac{81g^4}{8\lambda} \right) - \frac{g^2 m_H^2}{32\pi^2}. \quad (85)$$

We give the W-boson polarisation function at  $p^2 = -m_W^2$  in an even simpler form:

$$\begin{aligned} \Pi_W(-m_W^2) &= \frac{g^2 m_W^2}{96\pi^2} \left( \frac{59 + 3h^2}{2} \ln \frac{T^2}{m_W^2} + 21.188 - \frac{3h^2}{4} \right) \\ &\quad - \frac{g^2 m_W^2}{32\pi^2} \int_0^1 dx [-1 + (h^2 - 2)x + x^2] \ln[(1 - x)^2 + h^2 x] \\ &\quad + \frac{\lambda m_W^2}{24\pi^2} \left( 1 - \frac{1}{2} \ln \frac{T^2}{m_H^2} \right). \end{aligned} \quad (86)$$

## D Mixed 2-loop contribution to the potential energy density of the effective theory

'Figure 8' diagrams and thermal counterterm:

$$\frac{g^2}{2} \mathbf{AV} = 6g^2 \int \frac{1}{k^2 + m_{A0}^2} \int \frac{1}{Q^2 + m_a^2}$$

$$\begin{aligned}
& +3g^2 \int \frac{1}{k^2 + m_{A0}^2} \int \frac{Q_0^2}{Q^2(Q^2 + m_a^2)}, \\
\frac{g^2}{8}(\mathbf{AG} + \mathbf{AH}) &= \frac{3g^2}{8} \int \frac{1}{k^2 + m_{A0}^2} \left( 3 \int \frac{1}{Q^2 + m_G^2} + \int \frac{1}{Q^2 + m_H^2} \right), \\
-\frac{1}{2}m_D^2 \mathbf{A} &= -\frac{3}{2}m_D^2 \int \frac{1}{k^2 + m_{A0}^2}. \tag{87}
\end{aligned}$$

Here the integration signs refer either to 3-d momentum space integration over  $\mathbf{k}$ , or to finite T sum-integrals over Q.

*Mixed setting-sun diagrams:*

$$\begin{aligned}
\frac{g^2}{2} \mathbf{AVV} &= -6g^2 \int \frac{1}{(p^2 + m_{A0}^2)(Q^2 + m_a^2)(K^2 + m_a^2)} \\
&\quad \left( 2p^2 - 2\frac{(pk)^2}{K^2} + 2Q_0^2 + Q_0^2 \frac{(KQ)^2}{K^2 Q^2} \right), \\
\frac{g^2}{8} \mathbf{AHG} &= -\frac{3}{2}g^2 \int \frac{Q_0^2}{(p^2 + m_{A0}^2)(Q^2 + m_H^2)(K^2 + m_G^2)}, \\
\frac{g^2}{8} \mathbf{AGG} &= -\frac{3}{2}g^2 \int \frac{Q_0^2}{(p^2 + m_{A0}^2)(Q^2 + m_G^2)(K^2 + m_G^2)}, \\
-\frac{g^2}{8} \Phi_0^2 \mathbf{AVH} &= -\frac{3}{8}g^4 \Phi_0^2 \int \frac{1}{(p^2 + m_{A0}^2)(Q^2 + m_a^2)(K^2 + m_H^2)} \left( 1 - \frac{Q_0^2}{Q^2} \right), \\
\frac{g^2}{2} \mathbf{ACC} &= 3g^2 \int \frac{Q_0^2}{(p^2 + m_{A0}^2)Q^2 K^2}. \tag{88}
\end{aligned}$$

In these integrals the static momentum  $\mathbf{p}$  and the non-static momenta  $Q$  and  $K$  are related via  $\mathbf{p} + K + Q = 0$ .

## E Dependence of Feynman-integrals involving a static propagator on its mass

We analyze in Sections 4 and 5 integrals which are of the general form

$$\int_{\mathbf{p}} \frac{I(p^2)}{p^2 + m^2}, \tag{89}$$

where  $I(p^2)$  is the result of non-static sum-integrals. This function has a well-defined Taylor-series in  $\mathbf{p}^2$ , therefore one can form the following set of functions:

$$I_s(p^2) = I(p^2) - \sum_{i=0}^{s-1} \frac{p^{2i}}{i!} I^{(i)}(0), \quad I_0 \equiv I, \quad (90)$$

with  $I^{(i)}$  denoting the  $i$ -th derivative with respect to  $\mathbf{p}^2$ . The dependence of  $I(p^2)$  on the non-static mass-squares is also analytic, the coefficients of the corresponding series expansions are IR-finite.

Below we show that the part of the above integral depending non-analytically on  $m^2$  can be constructed explicitly. Namely, we prove, that

$$\int \frac{I(p^2)}{p^2 + m^2} = -\frac{m}{4\pi} I(p^2 = -m^2) + \sum_{s=0}^{\infty} (-m^2)^s \int \frac{I_s(p^2)}{p^{2(s+1)}}. \quad (91)$$

The first term on the right hand side is the explicit non-analytic piece, which can be interpreted as a factorised product of a static and of a non-static integral. The second term is IR-convergent.

The proof is based on the following identity:

$$\frac{I_s(p^2)}{p^{2(s+1)}(p^2 + m^2)} = \frac{I_{s+1}(p^2)}{p^{2(s+2)}} + \frac{I^{(s)}}{s!} \frac{1}{p^2(p^2 + m^2)} - m^2 \frac{I_{s+1}(p^2)}{p^{2(s+2)}(p^2 + m^2)} \quad (92)$$

This identity is applied repeatedly starting with the second term on the right hand side of the simple identity:

$$\frac{I(p^2)}{p^2 + m^2} = \frac{I(p^2)}{p^2} - m^2 \frac{I(p^2)}{p^2(p^2 + m^2)}. \quad (93)$$

Eventually, one arrives at the following representation of the integrand of (89):

$$\frac{I(p^2)}{p^2 + m^2} = \sum_{s=0}^{\infty} (-m^2)^s \frac{I_s(p^2)}{p^{2(s+1)}} - m^2 \sum_{s=0}^{\infty} (-m^2)^s \frac{I^{(s)}(0)}{s!} \frac{1}{p^2(p^2 + m^2)}. \quad (94)$$

The second term on the right hand side can be evaluated explicitly, when this equality is integrated with respect to  $\mathbf{p}$ . Also the  $s$ -sum in it can be done, leading to (91).

In our applications the integral we are interested in is a "mixed" static-non-static "setting sun". From its two vertices one has at least a factor  $g^2$ ,

therefore in an  $\mathcal{O}(g^4)$  accurate calculation one is satisfied with keeping the first few terms of the expansion (94) ( $m^2$  is of the order of  $g^2$ ):

$$\int_{\mathbf{p}} \frac{I(p^2)}{p^2 + m^2} = -\frac{m}{4\pi} I(0) + \int_{\mathbf{p}} \frac{I(p^2)}{p^2} - m^2 \int_{\mathbf{p}} \frac{I_1(p^2)}{p^4} + \mathcal{O}(g^5). \quad (95)$$

On the right hand side in the second term it is sufficient for the present accuracy to use the expansion of  $I(p^2)$  to linear order with respect to the non-static mass squares. In the third integral for the same purpose one simply sets these masses equal to zero.

## Acknowledgements

The authors are grateful to Z. Fodor, M. Laine, G. Mack, I. Montvay and J. Polonyi for valuable remarks, helpful criticism and encouragement.

## References

- [1] T. Appelquist and J. Carrazzone, Phys. Rev. **D11** (1975) 2856
- [2] S. Weinberg, Phys. Lett. **B91** (1980) 51
- [3] H. Georgi, Ann. Rev. Nucl. Part. Sci. **43** (1993) 209
- [4] E. Braaten, Phys. Rev. Lett. **74** (1995) 2164
- [5] for recent developments, see "Electroweak Physics and the Early Universe", Eds. J.C. Romao and F. Freire, NATO ASI Series B: Physics **338** (Plenum Press, 1995)
- [6] A. Jakovác, Phys. Rev. **D53** (1996) 4538
- [7] A. Kerres, G. Mack and G. Palma, Nucl. Phys. **B467** (1996) 510
- [8] K. Kajantie, M. Laine, K. Rummukainen and M. Shaposhnikov, Nucl. Phys. **B458** (1996) 90
- [9] K. Kajantie, M. Laine, K. Rummukainen and M. Shaposhnikov, Nucl. Phys. **B466** (1996) 189



- [10] A. Jakovác, A. Patkós and P. Petreczky, Phys. Lett. **B367** (1996) 283
- [11] P. Arnold and O. Espinosa, Phys. Rev. **D47** (1993) 3546
- [12] Z. Fodor and A. Hebecker, Nucl. Phys. **B432** (1994) 127
- [13] D. Bödeker, W. Buchmüller, Z. Fodor and T. Helbig, Nucl. Phys. **B423** (1994) 171
- [14] W. Buchmüller, Z. Fodor and A. Hebecker, Nucl. Phys. **B447** (1995) 317
- [15] K. Farakos, K. Kajantie, K. Rummukainen and M. Shaposhnikov, Nucl. Phys. **B425** (1994) 67
- [16] K. Kajantie, K. Rummukainen and M. Shaposhnikov, Nucl. Phys. **B407** (1993) 356
- [17] M. Losada, *High Temperature Dimensional Reduction of the MSSM and other Multi-Scalar Models*, Rutgers-preprint RU-96-25
- [18] J.M. Cline and K. Kainulainen, *Supersymmetric Electroweak Phase Transition Beyond Perturbation Theory* McGill-preprint, McGill/96-20
- [19] M. Laine, *Effective Theories of MSSM at High Temperatures* Heidelberg-preprint, HD-THEP-96-13
- [20] Z. Fodor, J. Hein, K. Jansen, A. Jaster and I. Montvay, Nucl. Phys. **B439** (1995) 147
- [21] F. Csikor and Z. Fodor, private communication
- [22] F. Karsch, T. Neuhaus, A. Patkós and J. Rank (in preparation)

### Tables

**Table 1:** Critical quantities from the non-polynomial, nonlocal approximation (NNA)

**Table 2:** Percentual variation of physical quantities relative to the NNA approximation. The symbols  $\delta_P$  and  $\delta_N$  refer to the  $(LPA - NNA)/LPA$  and  $(LNA - NNA)/LNA$  differences, respectively.

**Figure Captions**

**Figure 1:**  $T_c/M_H$  ratio as a function of  $M_H/M_W$  in NNA

**Figure 2:**  $\Phi_c/T_c$  ratio as a function of  $M_H/M_W$  in NNA

**Figure 3:**  $L_c/T_c^4$  ratio as a function of  $M_H/M_W$  in NNA

**Figure 4:** The surface tension ( $\sigma_c$ ) in  $(\text{GeV})^3$  units as a function of  $M_H/M_W$  in various approximations. **a:** NNA, **b:** LPA, **c:** LNA

$m_H^*$	$M_H$	$T_c/M_H$	$\Phi_c/T_c$	$\sigma_c/T_c^3$	$L_c/T_c^4$
30	26.72	2.35	2.336	0.1325	0.440
35	31.85	2.28	1.719	0.0634	0.257
40	36.96	2.23	1.333	0.0350	0.163
50	47.16	2.15	0.906	0.0146	0.081
60	57.28	2.08	0.687	0.0080	0.049
70	67.30	2.01	0.558	0.0051	0.034
80	77.23	1.95	0.476	0.0036	0.026
90	87.07	1.88	0.419	0.0028	0.020
100	96.81	1.82	0.378	0.0023	0.017
110	106.45	1.76	0.348	0.0019	0.015
120	115.99	1.71	0.325	0.0017	0.013

Table 1: Critical quantities from the non-polynomial, nonlocal approximation (NNA)

$m_H^*$	$\delta_P T_c$	$\delta_N T_c$	$\delta_P \Phi_c$	$\delta_N \Phi_c$	$\delta_P \sigma_c$	$\delta_N \sigma_c$	$\delta_P L_c$	$\delta_N L_c$
30	0.84	0.82	-2.25	-1.81	-6.19	-5.12	-6.29	-5.48
35	0.88	0.85	-1.89	-1.46	-4.50	-3.71	-5.69	-4.87
40	0.87	0.84	-1.38	-0.99	-3.15	-2.21	-4.73	-3.98
50	0.79	0.76	-0.49	-0.10	-0.95	-0.17	-3.10	-2.35
60	0.69	0.65	0.22	0.63	0.91	1.81	-2.04	-1.26
70	0.57	0.53	0.96	1.41	2.47	3.37	-1.22	-0.38
80	0.45	0.42	1.73	2.13	4.74	6.38	-0.64	0.09
90	0.33	0.30	2.61	3.05	6.99	8.55	-0.11	0.66
100	0.21	0.18	3.58	4.04	9.37	10.94	0.34	1.13
110	0.09	0.06	4.50	5.08	12.93	13.59	0.45	1.44
120	-0.02	-0.06	5.59	6.11	15.56	16.99	0.62	1.45

Table 2: Percentual variation of physical quantities relative to the NNA approximation. The symbols  $\delta_P$  and  $\delta_N$  refer to the  $(LPA - NNA)/LPA$  and  $(LNA - NNA)/LNA$  differences, respectively.

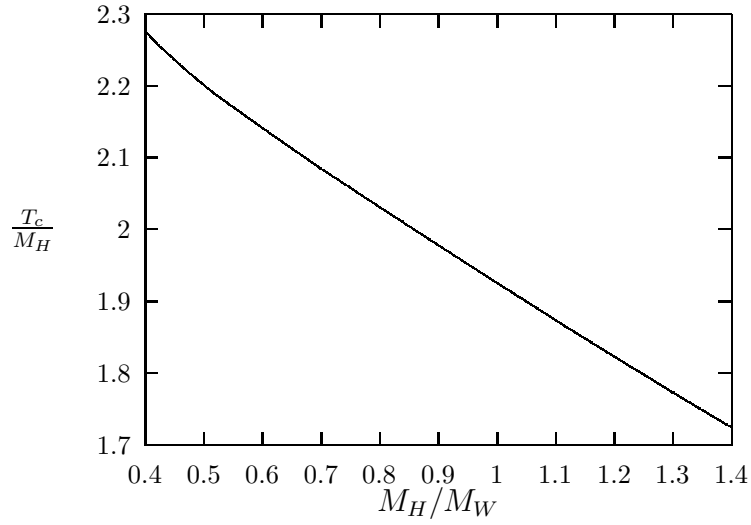


Figure 1:  $T_c/M_H$  ratio as a function of  $M_H/M_W$  in NNA

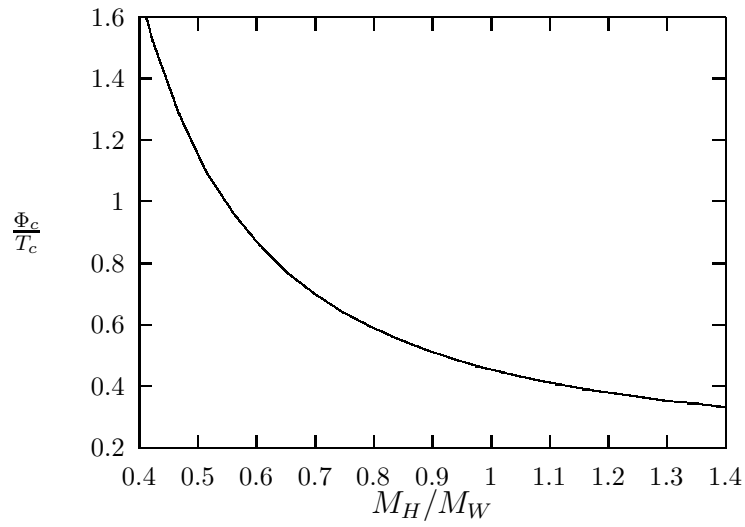


Figure 2:  $\Phi_c/T_c$  ratio as a function of  $M_H/M_W$  in NNA

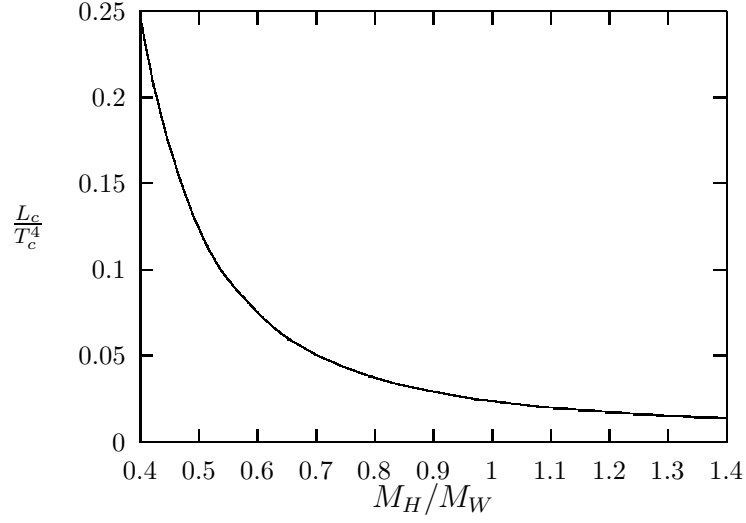


Figure 3:  $L_c/T_c^4$  ratio as a function of  $M_H/M_W$  in NNA

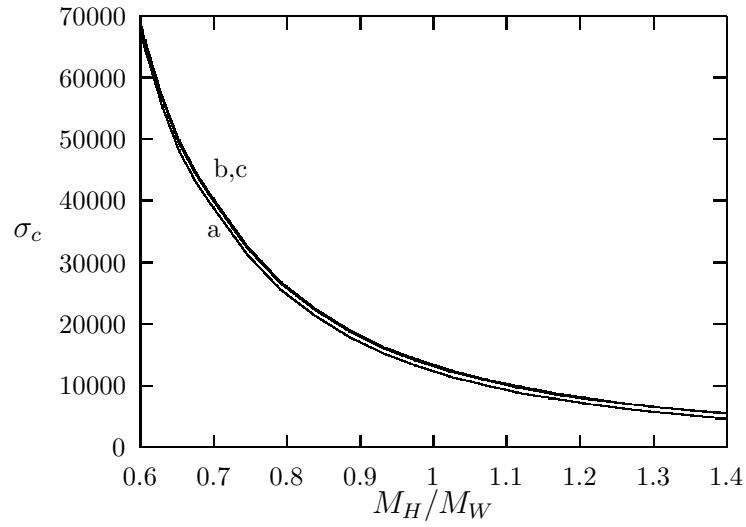


Figure 4: The surface tension ( $\sigma_c$ ) in  $(\text{GeV})^3$  units as a function of  $M_H/M_W$  in various approximations. **a**: NNA, **b**: LPA, **c**: LNA